Vol. 92 No. 3 pp. 1193–1217 ACTA GEOLOGICA SINICA (English Edition) June 2018

Geochemical Evaluation of the Permian Ecca Shale in Eastern Cape Province, South Africa: Implications for Shale Gas Potential

Christopher BAIYEGUNHI[1, *], Kuiwu LIU[1], Nicola WAGNER[2], Oswald GWAVAVA[1] and Temitope L. OLONINIYI[1]

1 *Department of Geology, University of Fort Hare, Private Bag X1314, Alice 5700, Eastern Cape Province, South Africa*

2 *Department of Geology, University of Johannesburg, PO Box 524, Auckland Park 2006, Johannesburg, South Africa*

Abstract: Shale gas has been the exploration focus for future energy supply in South Africa in recent time. Specifically, the Permian black shales of the Prince Albert, Whitehill, Collingham, Ripon and Fort Brown Formations are considered to be most prospective rocks for shale gas exploration. In this study, outcrop and core samples from the Ecca Group were analyzed to assess their total organic carbon (TOC), organic matter type, thermal maturity and hydrocarbon generation potential. These rocks have TOC ranging from 0.11 to 7.35 wt%. The genetic potential values vary from 0.09 to 0.53 mg HC/g, suggesting poor hydrocarbon generative potential. Most of the samples have Hydrogen Index (HI) values of less than 50 mg HC/g TOC, thus suggesting Type-IV kerogen. Tmax values range from 318ºC to 601ºC, perhaps indicating immature to over-maturity of the samples. The vitrinite reflectance values range from 2.22% to 3.93%, indicating over-maturity of samples. Binary plots of HI against Oxygen Index (OI), and HI versus Tmax show that the shales are of Type II and mixed Type II–III kerogen. Based on the geochemical data, the potential source rocks are inferred as immature to over-matured and having present-day potential to produce gas.

Key words: geochemistry, organic matter type, thermal maturity, hydrocarbons, Ecca Group, South Africa

1 Introduction

Shale gas equates to self-sourced, unconventional resources that are hosted or trapped in fine-grained and organic carbon-rich siliclastic sediments (Horsfield and Schulz, 2010). The natural gas can be generated in shale, but emanations from deeper subsurface can also contribute to the gas that is stored in the shale (Bustin et al., 2009). Shales are widely distributed in the world and only in the last two decades were they regarded as a potential source rock and/or seal/cap rock for conventional petroleum reservoirs. The last decade has marked an increase in the interest in natural gas, particularly from unconventional sources, as a 'cleaner' alternative and/or an additional source of energy generation. The depletion in conventional petroleum sources, and commercial production of shale gas in the United States have led to the realisation that organic-rich shale or fine-grained rocks can also serve as potential unconventional reservoirs for hydrocarbons (Curtis, 2002; Montgomery et al., 2005; Jarvie et al., 2007; Bilgen and Sarikaya, 2016). Presently, global petroleum exploration is undergoing a strategic shift from conventional to unconventional hydrocarbon resources. This development has led to a change in the way exploration companies, and geoscientists, consider resource plays. Shale-gas formations are now regarded as both source and reservoir rocks. The term 'shale' does not limit the gas host to only rock type shale, shale gas plays in variable facies are common (e.g. the Lewis Shale of the San Juan Basin in northwestern New Mexico and southwestern Colorado) and are well documented (Bustin et al., 2009). Natural gas produced and trapped within sedimentary facies such as mudrocks, carbonates and siltstones of extremely low permeability is also termed shale gas.

Source rock is one of the primary components of hydrocarbon system and thermal maturity is the main factor that determines whether a source rock can either

* Corresponding author. E-mail: cbaiyegunhi@ufh.ac.za

produce oil, gas, or condensate (Lecompte et al., 2010). Organic matter that is preserved in shales may change to oil and gas as temperature and pressure increases. The duration and degree of post-depositional burial are the two main parameters controlling the conversion of organic matter to natural gas. This gas may be trapped in the shale either as free gas in natural fractures and intergranular porosity, as gas sorbed into kerogen and clay-particle surfaces, or as gas dissolved in kerogen and bitumen (Curtis, 2002). Shale gas can be thermogenic or biogenic in origin as well as a combination of both (Curtis, 2002; Martini et al., 2008; Suarez-Ruiz et al., 2012; Bilgen and Sarikaya, 2016). Chemically, the gas can be dry, i.e. consisting over 90% methane, or wet, i.e. predominantly of longer chained hydrocarbons such as ethane and propane, etc.; however, a combination of the two is common.

Exploration for shale gas occurring in the formations of the Ecca Group started in the 1960s, but stopped in the late 1970s due to poor technical know-how (Cole, 1992; Branch et al., 2007). Presently, there is a renewed interest in the hydrocarbon-bearing potential of the lower Ecca Group shales in the Main Karoo Basin of South Africa (Geel et al., 2015). Recent analysis by Decker and Marot (2012) and Advanced Resources International (2013) revealed that the basin has potential gas reserves that range from 32–485 trillion cubic feet (Tcf) of technically recoverable shale gas resources and that most conservative prediction or likelihood is still an important gas resource. Kuuskraa et al. (2011) initially suggested an optimistic prospective area of about 183,000 km^2 with potential gas reserves of about 485 Tcf, making it the fifth largest in the world (Vermeulen, 2012). However, an area with a smaller extent of approximately 155,000 km^2 is now considered in relation to the thinning of the Karoo formations to the north and folding effects associated with the Cape Fold Belt (CFB), as well as the intrusion of dolerites (Geel et al., 2013; 2015). The more recent resource assessments indicate gas reserves ranging between 14 and 172 Tcf, with an average of approximately 40 Tcf (Business Day Live, 2014). Although, there was a substantial drop in the estimated recoverable reserves, the shale gas reserve is still considered to be feasible, especially when taking into account that the Moss gas project, which is currently the only gas exploration project in South Africa, was planned on a reserve of merely 3 Tcf (Vermeulen, 2012).

Exploration of the gas reserve has raised serious environmental concerns leading to arguments and a series of on-going debates. Supporters of shale gas exploration argue that it can help to meet the current and increasing future demands for energy, reduce dependency on coal-generated electricity, create jobs, and contribute to the mitigation of climate change or reduce environmental pollution (Cook et al., 2013; Council of Canadian Academies, 2014). However, those against shale gas exploration argue that hydraulic fracturing of the Karoo rocks for shale gas will contaminate the already scarce surface and groundwater resources as well as induce seismicity (Bipartisan Policy Center, 2012; Cook et al., 2013; Council of Canadian Academies, 2014; Du Toit and O'Connor, 2014; Vengosh et al., 2014). Presently, many states in the US have started to investigate the effects of hydraulic fracturing, while developing rules that will help to regulate the industry (Hackett et al., 2012). Nevertheless, the negative effects of fracking are highly contested by the extraction industries, and are still open to debate or in need of research (Zoback and Arent, 2014; Zou et al., 2016).

Unlike the basins in the US, the geology of the Main Karoo Basin is quite complex with intrusions of multiple dolerite sills and dykes at about 183 Ma (Chevallier and Woodford, 1999; Chevallier et al., 2001; Steyl and van Tonder, 2013). These dolerite intrusions might have impacted the quality of the shale resources and thus increase the risks of shale gas exploration. Nonetheless, the Ecca Group formations in the study area are thought to have a considerable carbon content and suitable thickness to make them an ideal target for shale gas development. According to Geel et al. (2015), the two main factors that affect the shale gas content and the distribution of gas are: (i) proximity of the host rocks to the south, near the CFB, and (ii) proximity of the host rocks to the north, where multiple dolerite intrusions exist, especially in the north of the southern Africa escarpment. They further documented that, in the first scenario, deformation and metamorphism of strata within the tectonic front of the CFB might perhaps have expelled most of the gas during the Cape Orogeny at about 276 Ma to 248 Ma (Hälbich, 1993; Hansma et al., 2015). In the second instance, contact metamorphism of gas-bearing strata adjacent or close to the dolerite intrusions related to the Karoo Large Igneous Province (Duncan et al., 1997) may have resulted in substantial gas loss due to thermal devolatization (Svensen et al., 2007; 2008). However, no loss of shale gas as a result of the aforementioned cases is reported here. To date, only sparse data exists on the geochemical characteristics of these Ecca Group formations.

In this study, the lower Ecca Group black shales in the Eastern Cape Province were geochemically evaluated to identify characteristics that would classify them as a potential resource for unconventional gas reservoir. Geographically, the study area lies between longitudes 24° E and 29° E and between latitudes 32°S and 34°S (Fig. 1).

2 Geology and Stratigraphy of the Main Karoo Basin

The Main Karoo Basin covers up to 700,000 km^2 of southern Africa and represents about 100 Ma of sedimentation spanning from 280 Ma to 180 Ma, reflecting periods of subsidence and sedimentation within the interior of Gondwana (Catuneanu et al., 2005; Johnson et al., 2006). The deposition of the Karoo sedimentary rocks occurred during the Late Carboniferous, and spans until the breakup of the African part of the Gondwana supercontinent during the Middle Jurassic at about 183 Ma (Johnson et al., 2006; Catuneanu et al., 2005; Johnson et al., 2006). This resulted in the building of the wide CFB thrust belt. Several researchers, such as De Wit and Ransome (1992), Catuneanu et al. (2005) and Johnson et al. (2006) have documented the Main Karoo Basin as a retro-arc foreland basin that developed in front of the CFB and behind an inferred magmatic arc that formed in response to shallow subduction of the Paleo-Pacific plate underneath Gondwana. However, Tankard et al. (2009) gave an alternative interpretation for the tectono-sedimentary evolution of the Karoo Basin by dividing it into a pre-foreland phase and a foreland phase. According to Tankard et al. (2009), the pre-foreland Karoo Basin that comprises of the Dwyka, Ecca and lower Beaufort Groups, developed within the continental interior of Gondwana due to vertical movement of rigid or firm blocks and intervening crustal faults. The foreland Karoo Basin (comprising the upper Beaufort Group) developed in response to the uplift of the CFB during the Early Triassic. Lindeque et al. (2011) and Pángaro and Ramos (2012) suggested that the CFB could be a (Jura-type) fold belt that developed as a result of arc–continent collision with subduction to the south, while the Karoo Basin formed as a flexure foreland basin to the CFB.

The northern part of the Main Karoo Basin rests unconformably on the Archean Kaapvaal Craton, whereas in the south, it conformably overlies the Cape Supergroup (Johnson et al., 2006; Tankard et al., 2009; 2012). In the south of the basin, strata of the Karoo Supergroup are deformed into mainly north-vergent structures in the area of the CFB (Johnson et al., 2006; Newton et al., 2006; Booth and Goedhardt, 2014), whereas in the interior of the basin, they are largely tabular and undeformed, pointing to the stability of the Kaapvaal Craton (Tankard et al., 2012). The Karoo Supergroup in the study area (Fig. 1) is composed of the basal glaciogenic Dwyka Group (Westphalian–Early Permian), the Permian marine Ecca Group, and the non-marine Beaufort Group (Permo-Triassic) (Johnson et al., 2006; Fildani et al., 2007). Stratigraphically, the Ecca Group can be subdivided into five formations, namely, the Prince Albert, Whitehill, Collingham, Ripon, and Fort Brown Formations (Johnson, 1976; SACS, 1980; Johnson et al., 1996; Figs. 1–2).

The Karoo Basin fill in the Eastern Cape Province started with the deposition of glacial sediments of the Dwyka Group in an extensive meltwater-fed lake, formed from glacio-marine deglaciation (Smith et al., 1993; Isbell et al., 2008). The initiation of the Dwyka sedimentation is estimated at about 300 Ma, following the 30 Ma stratigraphic breaks after the end of Viséan when sedimentation in the Cape Basin was terminated (Linol et al., 2015). The Dwyka Group unconformably overlies the Cape Supergroup in the south and is overlain by postglacial sediments of the Prince Albert Formation; these sediments were deposited through suspension settling of muds, starting at about 289 Ma (Cole, 2005; Tankard et al., 2012; Geel et al., 2013; 2015). Subsequently, carbonaceous shales of the Whitehill Formation that formed under anoxic conditions were deposited on the Prince Albert Formation (Cole, 2005; Geel et al., 2015). Conformably overlying the Whitehill Formation are fine-grained immature detrital mudstones, intercalated claystones and volcaniclastic tuffs, and lesser proportions of sandstone of the Collingham Formation (Wickens, 1994; Viljoen, 1992, 1994). Fildani et al. (2009) and McKay et al. (2015) documented that the age of deposition of the latter formation ranges between about 276 Ma and 268 Ma. Sedimentation in the overlying Ripon Formation continued in a marine setting, although with localized incursions of fluvial material. Later, the Fort Brown Formation, which is made up of sandstones alternating with shale, was deposited on the submarine shelf and deltas (Johnson, 1976). During the deposition of the Beaufort Group, the climate had warmed sufficiently to become semi-arid such that the Ecca seaway regressed. This led to the establishment of a fully non-marine environment and resulted in the accumulation of the fluvio-lacustrine Beaufort Group (Johnson et al., 2006). The transition into terrestrial from marine environments marks the boundary between the Ecca and Beaufort Groups that occurred over a period of about 30 Ma (270 Ma to 240 Ma). Johnson et al. (2006) discerned that subsequent orogenic activity at the beginning of the Triassic with associated uplift resulted in the influx of Beaufort sediments, which extended throughout the basin. The overlying Late Triassic–Early Jurassic Stormberg Group was deposited as a result of the final deformational phase in the CFB (Hälbich et al., 1983). The Stormberg Group comprises fluvial and aeolian-lacustrine successions of the Molteno, Elliot and Clarens Formations (Johnson et al., 1996). The whole sequence of deposition is covered by the basaltic and pyroclastic deposits of the Drakensberg Group (Johnson et al., 2006; Rubidge et al., 2013).

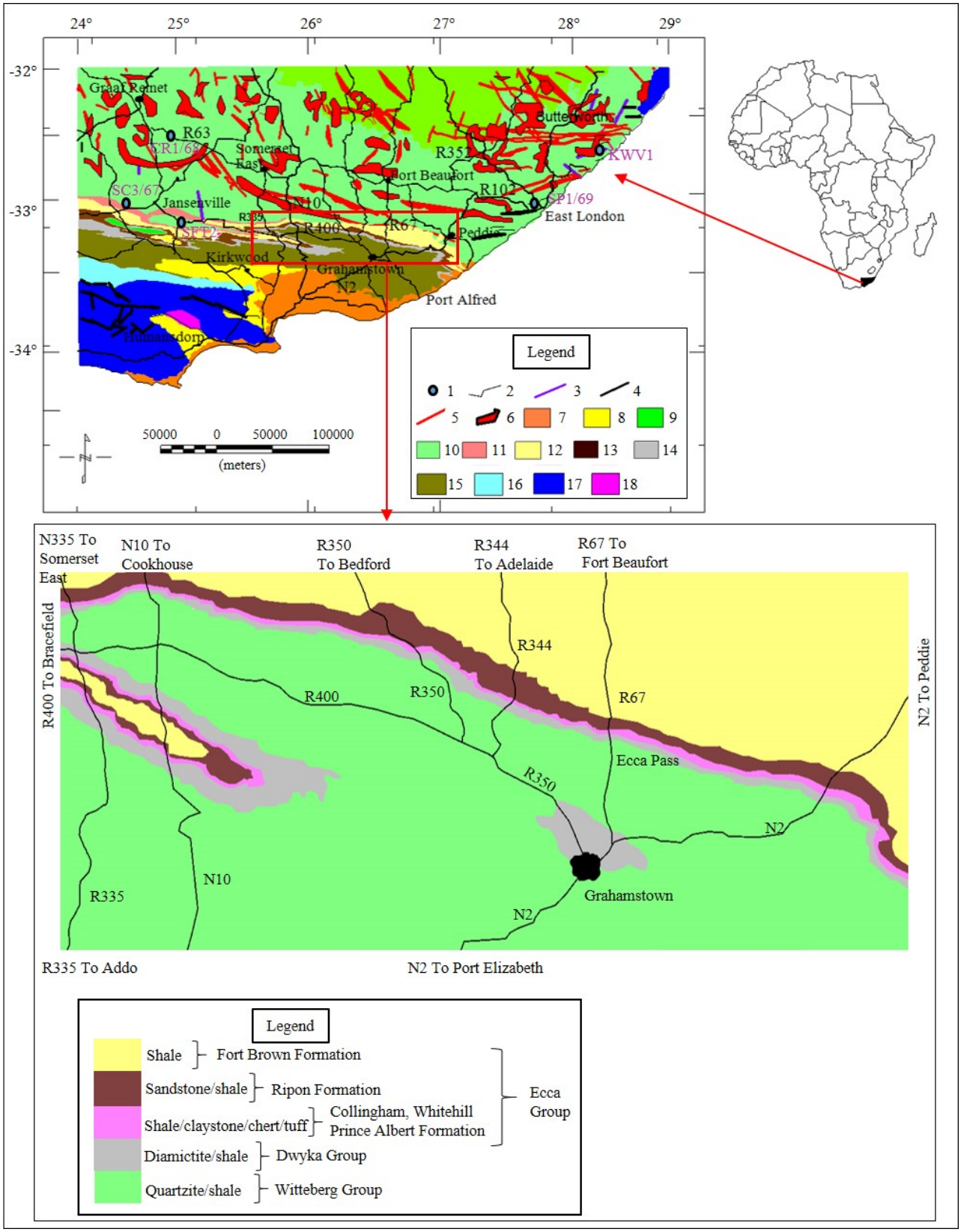

Fig. 1. Geological map of the study area (modified from Johnson et al., 1996, 2006).

In the insert map: 1, norehole; 2, road; 3, lineament; 4, fault; 5, dolerite dyke; 6, dolerite sill; 7, Cenozoic deposits; 8, Uitenhage and Zululand Groups; 9, Tarkastad Subgroup; 10, Adelaide Subgroup; 11, Waterford Formation; 12, Fort Brown Formation; 13, Collingham, Whitehill and Prince Albert Formations; 14, Dwyka Group; 15, Witteberg Group; 16, Bokkeveld Group; 17, Table Mountain and Natal Groups; 18, Malmesburg, Kaaismans, Gamboos and Congo Caves Groups.

Supergroup	Group	Subgroup	Formation	Member	Lithology	Maximum thickness (m)
Karoo			Drakensberg		Basalt, Pyroclastic deposits	1400
			Clarens		Sandstone	300
			Elliot		Mudstone, Sandstone	500
			Molteno		Sandstone, Shale, coal	450
	Beaufort	Tarkastad	Burgersdorp		Mudstone, Sandstone, Shale	1000
			Katberg	Palingkloof	Mudstone, Sandstone, Shale	900
		Adelaide	Balfour	Palingkloof	Mudstone, Sandstone, Shale	50
				Elandsberg	Sandstone, Silt	700
				Barberskrans	Sandstone, Shale	100
				Daggaboersnek	Sandstone, Silt, Shale	1200
				Oudeberg	Sandstone, Shale	100
			Middleton		Sandstone, Shale, Mudstone	1500
			Koonap		Sandstone, Shale	1300
	Ecca		Waterford		Sandstone, Shale	800
			Fort Brown		Shale, Sandstone	1500
			Ripon		Sandstone, Shale	1000
			Collingham		Shale, Claystone	30
			Whitehill		Black Shale, Chert	70
			Prince Albert		Khaki Shale	120
			Dwyka		Diamictite, Tillite, Shale	750

Fig. 2. Lithostratigraphy of the Karoo Supergroup in the Eastern Cape Province, as compiled by the Council for Geoscience (after Johnson et al., 2006).

3 Material and Methods

3.1 Materials

A total of 82 outcrop samples of shale presumed to be rich in organic matter were collected from road-cut exposures of the Ecca Group along Regional roads R67 (Ecca Pass; Grahamstown–Fort Beaufort), R344 (Grahamstown–Adelaide), R350 (North of Kirkwood–Somerset East), and National roads N2 (Grahamstown–Peddie), and N10 (Paterson–Cookhouse) for source rock

analysis (Fig. 1). In addition, 38 core samples of Ecca shale from boreholes CR1/68, SC3/67, SP1/69 and KWV1 were collected from the Council for Geosciences core library in Pretoria, making a total of 120 shale samples that were tested for TOC content. A total of 28 shale samples from boreholes SP1/69 and KWV1 were further analyzed.

3.2 Methods

3.2.1 Total organic carbon content (TOC)

Samples for TOC determination were cleaned, crushed and milled to fine powder form, passing through a 60-mesh (250 μm) sieve; 20 g of each sample was accurately weighed into clean LECO crucibles. The shale samples were then de-mineralized by adding hot 10 % hydrochloric acid and afterwards distilled water was added to halt the reaction. The acid was removed from the sample using a filtration apparatus fitted to a glass microfiber filter. Thereafter, the samples were dried in an oven at 60ºC for 24 hours. The dried samples were weighed and then introduced into a muffle furnace at 650ºC for combustion. After combustion, the samples were allowed to cool down and re-weighed to determine the TOC content. Samples that have TOC value above 0.5wt% are considered to be source rocks and termed adequate, whereas those with TOC below 0.5 wt% are termed inadequate because they do not reflect as source rocks (Tissot and Welte, 1978). The shale samples that are adequate (TOC value >0.5 wt%) were further analysed for vitrinite reflectance and rock-eval pyrolysis (see below and Table 1).

3.2.2 Rock-eval pyrolysis

Twenty-eight organic-rich shale samples were analysed using the Rock-Eval-6 pyrolyser at the GeoMark Research Laboratory, Houston, Texas in the United States to determine the hydrocarbon generation potential, maturity, kerogen type and hydrogen richness. The samples were cleaned, crushed, weighed accurately in a sample holder and heated in an inert atmosphere to 600ºC using a special temperature programme. The samples were initially heated at 300ºC for 3 mins to generate the first peak (S1), which represents free and adsorptive hydrocarbon in the sample. This was followed immediately by programmed pyrolysis as the oven temperature was ramped up rapidly to 600ºC at the rate of 25ºC/min to give the second peak (S2). S2 represents hydrocarbon generated during thermal cracking of kerogen. Simultaneously, the CO_2 produced during the temperature interval was recorded as the third peak (S3). Both the S1 and S2 hydrocarbon peaks were measured by the flame ionization detector (FID). The splitting arrangement allows measurement of S3 (carbon dioxide) by means of a thermal conductivity detector (TCD). Tmax, which is the temperature that corresponds to the maximum S2 peak was obtained from the instrument (Fig. 3). Other parameters like hydrocarbon potential (SP), production index (PI), hydrogen index (HI) and oxygen index (OI) were calculated.

In this study, rock-eval data were interpreted based on guidelines documented by Tissot and Welte (1984), Peters

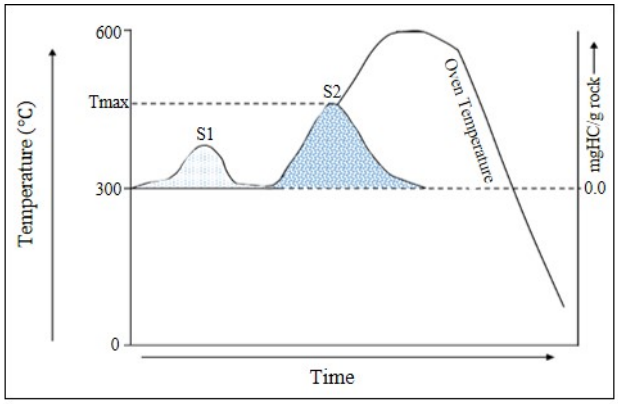

Fig. 3. Response of organic matter to controlled heating during pyrolysis. S1 corresponds to hydrocarbons formed in the sub-surface and already present in the rock, whereas S2 represents hydrocarbons generated during the pyrolysis process. Tmax corresponds to the maximum generation of hydrocarbons during pyrolysis and is much higher that the temperature governing the formation of hydrocarbons in nature (from Barker, 1996 and Ferreira 2014).

Table 1 Measured and calculated parameters derived from rock-eval pyrolysis (after Ferreira, 2014)

	Parameters
Measured	S_1 = hydrocarbons thermally distilled from the whole rock at temperature < 300°C. Units: mg of hydrocarbon/gram of rock S_2 = hydrocarbons generated by pyrolytic degradation of kerogen between 300 and 650°C. Units: mg of hydrocarbon /gram of rock S_3 = a measure of organic CO_2 generated between temperature of 300 and 390°C. Units: mg of CO_2/gram of rock
Calculated	SP (hydrocarbon potential) = $S_1 + S_2$ SP indicates the total amount of hydrocarbons that the source rock, at matured level, can generate. Thus accounts for free hydrocarbons in the source rock (S1) and these hydrocarbons can still produce with increased maturation (S2) (McCarthy et al., 2011). PI (production index) = $S_1/(S_1 + S_2)$ PI is used to characterise the evolution of the organic matter as PI increases with depth in very fine grained rocks, also with source rock maturation before hydrocarbon are expelled (McCarthy et al., 2011). HI (hydrogen index) = $(S_2/TOC) \times 100$ HI is proportional to the amount of hydrogen contained within the kerogen, with higher HI indicating a potential for oil production (McCarthy et al., 2011). OI (oxygen index) = $(S_3/TOC) \times 100$ OI is related to the amount of oxygen in the kerogen and useful to in tracking the maturation path of the kerogen (McCarthy et al., 2011). It is generally higher in kerogen derived from terrestrial sources.

(1986), and Nuñez-Betelu and Baceta (1994), which utilized graphs of various parameters in addition to evaluating the appropriate parameters individually. Petrophysical properties (i.e. porosity, permeability and density) of the Ecca shales in boreholes KWV1 and SP1/69 were extracted from the borehole log sheets and used for comparison.

3.2.3 Vitrinite Reflectance (RO)

Nineteen out of the 28 organic-rich shale samples were analysed for vitrinite reflectance. Three samples originate from borehole SP1/69 (small chips) and 16 samples are from borehole KWV1. Samples were taken from different horizons in the Ripon, Collingham, Whitehill, and Prince Albert Formations (Figs. 1, 4 and 5). The chips or portions of core samples were prepared perpendicular to the bedding plane in order to observe particles embedded vertically. The samples were mounted in epoxy resin, ground and polished in accordance with South African National Standard (SANS ISO 7404-2). Random reflectance at 546 nm using immersion oil and total magnification of x500 in non-polarised light were conducted following the American Society for Testing and Materials (ASTM) ASTM D7708-14 (microsocial

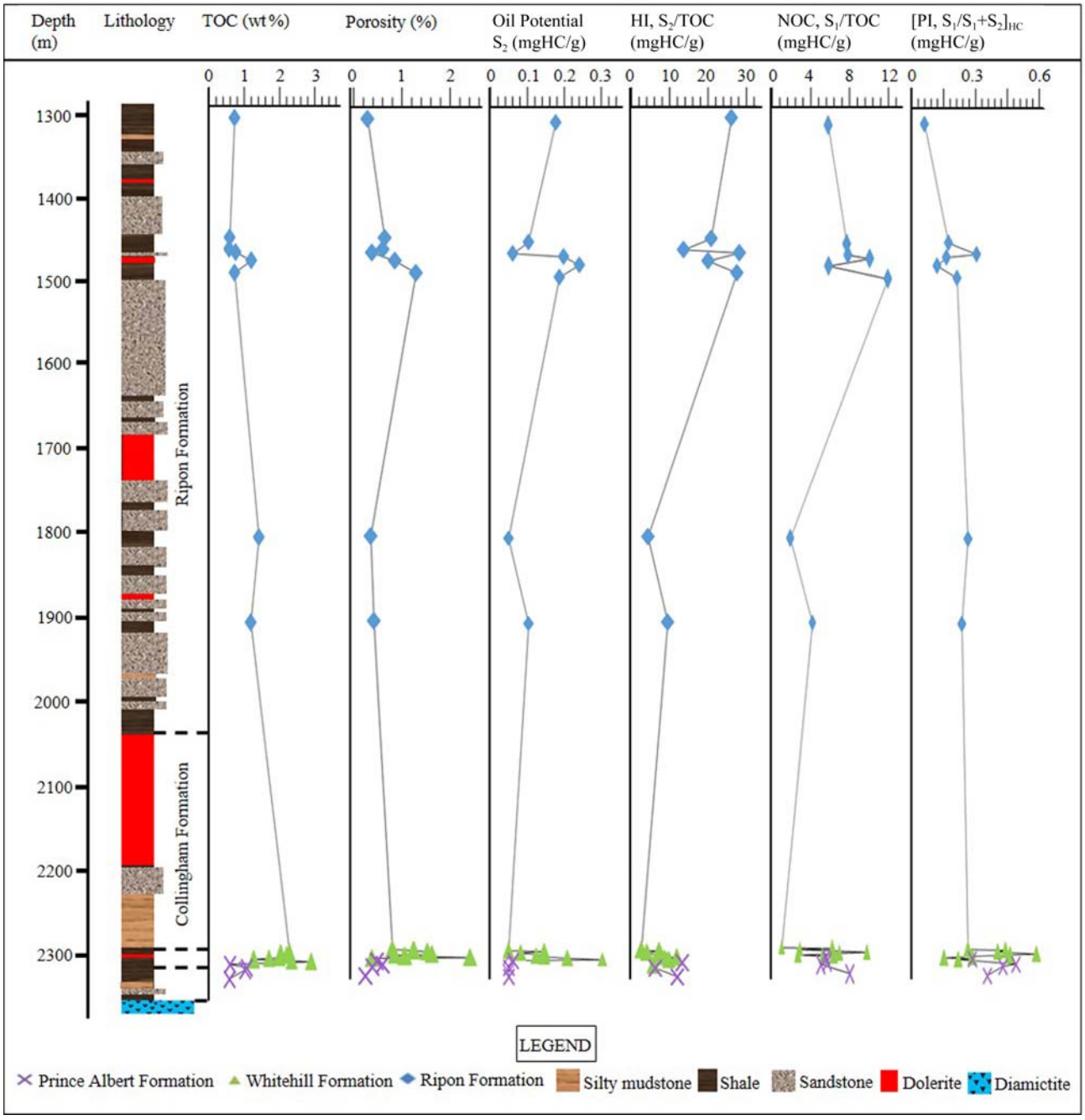

Fig. 4. Downhole TOC, porosity, oil potential, hydrogen index, normal oil content, and production index for borehole KWV1.

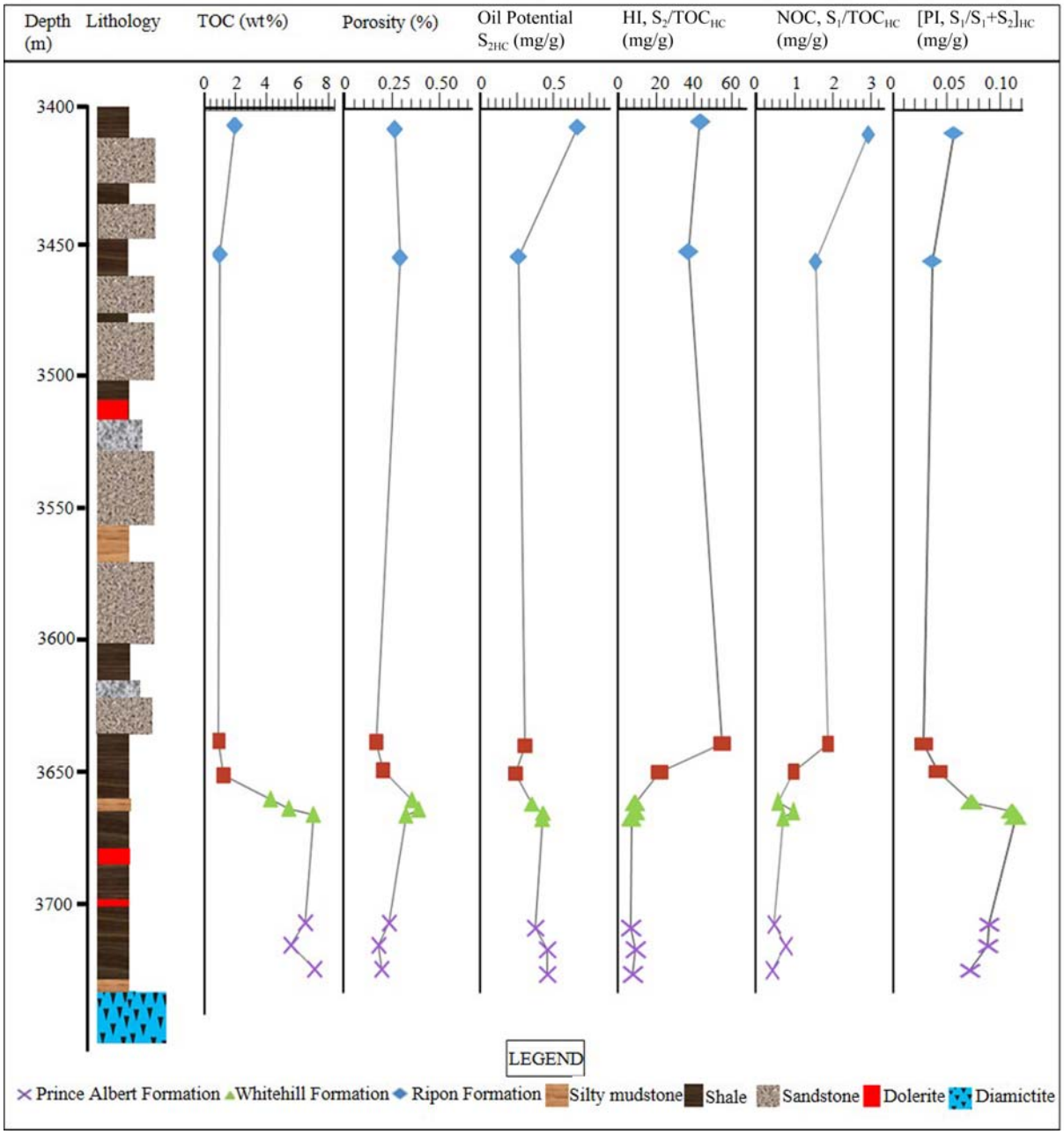

Fig. 5. Downhole TOC, porosity, oil potential, hydrogen index, normal oil content, and production index for borehole SP1/69.

determination of the reflectance of vitrinite in sedimentary rocks). The analysis was conducted on a Zeiss AxioImager reflected light microscope fitted with Hilgers Diskus software for vitrinite reflectance determination. The equipment was calibrated following South African National Standard (SANS ISO 7404-5) and ASTM D7708-14, using calibration standards YAG 0.900, and CZ 3.24. Twenty to 50 readings were taken on each sample across the surface at a magnification of x500. In order to accurately determine the organic matter, the samples were viewed under white light (monochromatic and colour cameras), in fluorescent mode (to determine degree of fluorescence), and under x-polars (to determine degree of anisotropy).

4 Results and Discussion

4.1 Total organic carbon (TOC) content

The Ecca shales have TOC values ranging from 0.11 to 7.35 wt% (Table 2; Figs. 4, 5). The obtained data for the outcrop and core samples show that the TOC values are between 0.17 and 7.35 wt%, 0.11 and 7.30 wt%, 0.22 and 0.93 wt%, 0.17 and 2.62 wt%, and 0.31 and 0.45 wt% for the Prince Albert, Whitehill, Collingham, Ripon and Fort

Table 2 Results of TOC analysis of shale samples from the Ecca Group

S. ID	Sample type	Formation	TOC	S. ID	Sample type	Formation	TOC
FB5	Outcrop (G-F)	Fort Brown	0.45	WK8	Core (KWV1)	Whitehill	2.36
FB4	Outcrop (G-F)	Fort Brown	0.34	WK7	Core (KWV1)	Whitehill	2.07
FB3	Outcrop (G-F)	Fort Brown	0.37	WK6	Core (KWV1)	Whitehill	2.28
FB2	Outcrop (G-F)	Fort Brown	0.31	WK5	Core (KWV1)	Whitehill	2.06
FB1	Outcrop (G-F)	Fort Brown	0.39	WK4	Core (KWV1)	Whitehill	1.72
RK6	Core (KWV1)	Ripon	0.68	WK3	Core (KWV1)	Whitehill	1.25
RK5	Core (KWV1)	Ripon	0.52	WK2	Core (KWV1)	Whitehill	2.42
RK4	Core (KWV1)	Ripon	0.51	WK1	Core (KWV1)	Whitehill	3.02
RK3	Core (KWV1)	Ripon	0.70	WS3	Core (SP1/69)	Whitehill	4.30
RK2	Core (KWV1)	Ripon	1.18	WS2	Core (SP1/69)	Whitehill	5.60
RK1	Core (KWV1)	Ripon	0.68	WS1	Core (SP1/69)	Whitehill	7.30
RS2	Core (SP1/69)	Ripon	1.72	WC3	Core (CR1/68)	Whitehill	0.37
RS1	Core (SP1/69)	Ripon	2.62	WC2	Core (CR 1/68)	Whitehill	0.52
RC3	Core (CR1/68)	Ripon	0.32	WC1	Core (CR 1/68)	Whitehill	0.48
RC2	Core (CR 1/68)	Ripon	0.31	WSC4	Core (SC 3/67)	Whitehill	0.44
RC1	Core (CR 1/68)	Ripon	0.48	WSC3	Core (SC 3/67)	Whitehill	0.45
RSC3	Core (SC 3/67)	Ripon	0.46	WSC2	Core (SC 3/67)	Whitehill	0.22
RSC2	Core (SC 3/67)	Ripon	0.27	WSC1	Core (SC 3/67)	Whitehill	0.31
RSC1	Core (SC 3/67)	Ripon	0.41	WH19	Outcrop (G-F)	Whitehill	0.36
RP24	Outcrop (G-F)	Ripon	0.28	WH18	Outcrop (G-F)	Whitehill	0.43
RP23	Outcrop (G-F)	Ripon	0.48	WH17	Outcrop (G-F)	Whitehill	0.51
RP22	Outcrop (G-F)	Ripon	0.39	WH16	Outcrop (G-F)	Whitehill	0.62
RP21	Outcrop (G-F)	Ripon	0.47	WH15	Outcrop (G-F)	Whitehill	0.40
RP20	Outcrop (G-F)	Ripon	0.46	WH14	Outcrop (G-F)	Whitehill	0.36
RP19	Outcrop (G-F)	Ripon	0.40	WH13	Outcrop (G-P)	Whitehill	0.20
RP18	Outcrop (G-F)	Ripon	0.37	WH12	Outcrop (G-P)	Whitehill	0.24
RP17	Outcrop (G-F)	Ripon	0.50	WH11	Outcrop (G-P)	Whitehill	0.37
RP16	Outcrop (G-F)	Ripon	0.38	WH10	Outcrop (G-P)	Whitehill	0.11
RP15	Outcrop (G-P)	Ripon	0.29	WH9	Outcrop (G-P)	Whitehill	0.42
RP14	Outcrop (G-P)	Ripon	0.43	WH8	Outcrop (C-P)	Whitehill	0.35
RP13	Outcrop (G-P)	Ripon	0.34	WH7	Outcrop (C-P)	Whitehill	0.38
RP12	Outcrop (G-P)	Ripon	0.44	WH6	Outcrop (C-P)	Whitehill	0.29
RP11	Outcrop (C-P)	Ripon	0.39	WH5	Outcrop (C-P)	Whitehill	0.24
RP10	Outcrop (C-P)	Ripon	0.49	WH4	Outcrop (G-A)	Whitehill	0.38
RP9	Outcrop (C-P)	Ripon	0.47	WH3	Outcrop (G-A)	Whitehill	0.46
RP8	Outcrop (C-P)	Ripon	0.40	WH2	Outcrop (G-A)	Whitehill	0.43
RP7	Outcrop (C-P)	Ripon	0.28	WH1	Outcrop (G-A)	Whitehill	0.39
RP6	Outcrop (G-A)	Ripon	0.31	PK4	Core (KWV1)	Prince Albert	0.53
RP5	Outcrop (G-A)	Ripon	0.45	PK3	Core (KWV1)	Prince Albert	1.04
RP4	Outcrop (G-A)	Ripon	0.44	PK2	Core (KWV1)	Prince Albert	0.98
RP3	Outcrop (G-A)	Ripon	0.35	PK1	Core (KWV1)	Prince Albert	0.50
RP2	Outcrop (G-A)	Ripon	0.42	PS3	Core (SP1/69)	Prince Albert	6.73
RP	Outcrop (G-A)	Ripon	0.33	PS2	Core (SP1/69)	Prince Albert	5.71
RP1	Outcrop (G-A)	Ripon	0.37	PS1	Core (SP1/69)	Prince Albert	7.35
CS2	Core (SP1/69)	Collingham	0.52	PC2	Core (CR 1/68)	Prince Albert	0.52
CS1	Core (SP1/69)	Collingham	0.93	PC1	Core (CR 1/68)	Prince Albert	0.49
CC2	Core (CR 1/68)	Collingham	0.44	PSC2	Core (SC 3/67)	Prince Albert	0.53
CC1	Core (CR 1/68)	Collingham	0.30	PSC1	Core (SC 3/67)	Prince Albert	0.17
CSC2	Core (SC 3/67)	Collingham	0.40	PA12	Outcrop (G-F)	Prince Albert	0.42
CSC1	Core (SC 3/67)	Collingham	0.34	PA11	Outcrop (G-F)	Prince Albert	0.44
CH10	Outcrop (G-F)	Collingham	0.27	PA10	Outcrop (G-F)	Prince Albert	0.31
CH9	Outcrop (G-F)	Collingham	0.36	PA9	Outcrop (G-F)	Prince Albert	0.42
CH8	Outcrop (G-F)	Collingham	0.49	PA8	Outcrop (G-P)	Prince Albert	0.46
CH7	Outcrop (G-P)	Collingham	0.50	PA7	Outcrop (G-P)	Prince Albert	0.49
CH6	Outcrop (G-P)	Collingham	0.39	PA6	Outcrop (G-P)	Prince Albert	0.28
CH5	Outcrop (G-P)	Collingham	0.37	PA5	Outcrop (C-P)	Prince Albert	0.37
CH4	Outcrop (G-A)	Collingham	0.30	PA4	Outcrop (C-P)	Prince Albert	0.33
CH3	Outcrop (G-A)	Collingham	0.22	PA3	Outcrop (G-A)	Prince Albert	0.45
CH2	Outcrop (G-A)	Collingham	0.28	PA2	Outcrop (G-A)	Prince Albert	0.38
CH1	Outcrop (G-A)	Collingham	0.24	PA1	Outcrop (G-A)	Prince Albert	0.47

Brown Formations, respectively. Along the Ecca Pass, the calculated average TOC value (i.e. 1.5 wt%) for the Whitehill Formation is higher than those of the underlying Prince Albert Formation and overlying Collingham and Ripon Formations. Thus, it can be inferred that the Whitehill Formation is more organically rich than the underlying and overlying formations at this location. Along Grahamstown–Peddie, where the lower Ecca formations are intruded by dolerites, the TOC values range from 0.17 to 0.62 wt%, with an average of 0.35 wt%. The TOC values are significantly lower than those obtained along the Ecca Pass (without dolerite intrusions on the surface).

In borehole SP1/69 (located near East London; Fig. 1),

the average (TOC) content in the shale of Prince Albert, Whitehill, Collingham and Ripon Formations are 6.6 wt%, 5.7 wt%, 0.7 wt%, and 2.2wt.%, respectively. These TOC values are generally higher than 2.0 wt% and such levels of organic enrichment are considered to represent good source rocks for hydrocarbon generation (Hedberg and Moody, 1979; Hunt, 1979; Peters and Cassa, 1994). On the other hand, at borehole KWV1 (located near Butterworth; Fig. 1), the average TOC values of the Prince Albert, Whitehill and Ripon shales are 0.77 wt%, 2.14 wt%, and 0.85 wt%, respectively, indicating a fair–good source rock. Generally, the average TOC values of the Ecca shales in borehole SP1/69 are higher than those in KWV1, suggesting that the hydrocarbon potential for the Ecca lithofacies in the East London area is better than in the Butterworth area (Fig. 1).

In both outcrop and boreholes samples, the TOC values tend to be smaller in samples that are within areas intruded by dolerites or close to dolerite intrusions. The impact of dolerite intrusions could possibly have reduced the TOC content in the host rock and thus areas that are intruded by dolerites are unlikely to be good shale gas reservoirs. Summary of the petrophysical properties of the Ecca Group rocks is presented in Table 3.

4.2 Quality and type of organic matter

The organic matter type is a vital parameter to be considered when evaluating source rock potential because it significantly influences the nature of hydrocarbon products (Hunt, 1979; Tissot and Welte, 1984; Barker, 1996). The type of organic matter gives insight into the depositional environment of the source rock and aids in predicting the generative potential of oil and gas. Organic matter types can be categorized into Types I, II, III and IV kerogen using bivariate plots of HI vs Tmax, S2 vs TOC, and HI vs OI. In the HI vs. OI classification diagram, known as a Van Krevelen diagram, the source rocks are analysed for kerogen using known evolution paths for different kerogen types (Peters, 1986). Generally, an HI value of more than 600 mg HC/g TOC indicates the predominance of Type I kerogen and this has potential to produce oil (Peters and Cassa, 1994). Type I kerogen is derived mainly from algae and associated with lacustrine depositional settings (McCarthy et al., 2011). Type II kerogen is associated with the production of oil, with HI values ranging between 300 mg HC/g TOC and 600 mg HC/g TOC (Peters and Cassa, 1994). The Type II kerogen is primarily derived from plankton, with some contribution from algal material, thus point to a marine depositional setting (McCarthy et al., 2011). HI values varying from 200 mg HC/g TOC to 300 mg HC/g TOC suggest a mix of Types II and III kerogen, expected to produce a mix of oil and gas (Peters and Cassa, 1994). Marine environments with significant terrestrial input, and vice versa, are the likely depositional environments for this type of organic matter. A shallow marine environment can receive terrestrial input, especially during sea level regression, and is a suitable example for the deposition of a mixed kerogen type. HI values between 50 mg HC/g TOC and 200 mg HC/g TOC are usually associated with Type III kerogen, which is mainly derived from higher plants and produces gas when matured. Type IV kerogen has HI values of less than 50 mg HC/g TOC and McCarthy et al. (2011) documented that such a kerogen type is mostly derived from reworked organic matter (mainly dead carbon) with little or no potential for hydrocarbon generation.

The results of the rock-eval analyses of shale samples from borehole KWV1 and SP1/69 are presented in Table 4. Based on the classification schemes of Peters and Cassa (1994) and McCarthy et al. (2011), with the exception of one sample from the Collingham Formation (sample CS2), all other samples have HI values of less than 50 mg HC/g TOC, thus suggesting Type-IV kerogen and these are mostly derived from reworked organic matter (mainly dead carbon) with little or no potential for hydrocarbon (dry gas) generation. On the other hand, S2/S3 values for the shales range between 0.4 and 7.5, indicating mixed types II/III, III, and IV kerogen that are expected to produce mixed oil and gas, and gas (Table 5; after Peters and Cassa, 1994). In addition, most of the samples have S1 and S2 values below 0.5 and 2.5, respectively, indicating poor quality of the organic matter (Table 6; after Peters, 1986). The plot of HI against OI (modified Van Krevelen diagram) and HI versus Tmax shows that the samples are of Type II and mixed Type II–III

Table 3 Petrophysical properties of the Ecca Group rocks in the study area

Formation	Lithology	Average thickness (m)	Average density (kg/m^3)	Average porosity (%)	Average permeability (mD)
Fort Brown	Sandstone	892	2.774	0.444	0.042
	Shale		2.656	0.574	0.032
Ripon	Sandstone	700	2.721	1.241	0.024
	Shale		2.662	0.595	0.046
Collingham	Shale	65	2.598	0.388	0.018
Whitehill	Shale	21	2.526	2.310	0.892
Prince Albert	Shale	87	2.641	0.560	0.014

Table 4 Results of Rock-Eval analysis of shale samples from borehole KWV1 and SP1/69

S. ID	Sample type	Formation	TOC	S1	S2	S3	S2/S3	HI	OI	Tmax	Ro_c	Ro_m
RK6	Core (KWV1)	Ripon	0.68	0.04	0.18	0.04	4.50	26	6	456	3.32	-
RK5	Core (KWV1)	Ripon	0.52	0.04	0.11	0.03	3.67	21	6	447	3.20	-
RK4	Core (KWV1)	Ripon	0.51	0.04	0.07	0.03	2.33	14	6	430	3.18	-
RK3	Core (KWV1)	Ripon	0.70	0.07	0.2	0.08	2.50	29	11	488	3.49	*
RK2	Core (KWV1)	Ripon	1.18	0.07	0.24	0.16	1.50	20	14	481	3.48	-
RK1	Core (KWV1)	Ripon	0.68	0.08	0.19	0.09	2.11	28	13	483	3.42	-
RS2	Core (SP1/69)	Ripon	1.72	0.05	0.75	0.34	2.21	44	20	460	3.26	-
RS1	Core (SP1/69)	Ripon	2.62	0.01	0.23	0.14	1.64	37	22	492	3.56	*
CS2	Core (SP1/69)	Collingham	0.52	0.01	0.29	0.20	1.45	53	36	513	3.67	*
CS1	Core (SP1/69)	Collingham	0.93	0.01	0.20	0.79	0.25	21	83	599	3.89	-
WK8	Core (KWV1)	Whitehill	2.36	0.03	0.06	0.04	1.5	3	2	405	3.05	3.44
WK7	Core (KWV1)	Whitehill	2.07	0.13	0.15	0.04	3.75	7	2	334	2.82	3.55
WK6	Core (KWV1)	Whitehill	2.28	0.07	0.09	0.06	1.50	4	3	333	2.79	3.49
WK5	Core (KWV1)	Whitehill	2.06	0.2	0.15	0.1	1.50	7	5	320	2.70	3.69
WK4	Core (KWV1)	Whitehill	1.72	0.12	0.13	0.06	2.17	8	3	318	2.61	2.22
WK3	Core (KWV1)	Whitehill	1.25	0.08	0.15	0.02	7.50	12	2	385	3.24	*
WK2	Core (KWV1)	Whitehill	2.42	0.07	0.21	0.1	2.10	9	4	408	3.07	3.24
WK1	Core (KWV1)	Whitehill	3.02	0.16	0.3	0.18	1.67	10	6	411	3.10	3.53
WS3	Core (SP1/69)	Whitehill	4.30	0.03	0.35	0.25	1.40	8	6	524	3.61	*
WS2	Core (SP1/69)	Whitehill	5.60	0.06	0.45	0.66	0.68	8	12	568	3.75	-
WS1	Core (SP1/69)	Whitehill	7.30	0.06	0.44	0.79	0.56	6	11	601	3.93	-
PK4	Core (KWV1)	Prince Albert	0.53	0.03	0.07	0.03	2.33	13	6	421	3.13	*
PK3	Core (KWV1)	Prince Albert	1.04	0.06	0.06	0.14	0.43	6	13	429	3.17	-
PK2	Core (KWV1)	Prince Albert	0.98	0.05	0.06	0.15	0.40	6	15	425	3.15	-
PK1	Core (KWV1)	Prince Albert	0.50	0.04	0.06	0.02	3.00	12	4	415	3.12	*
PS3	Core (SP1/69)	Prince Albert	6.73	0.04	0.38	0.34	1.12	6	5	590	3.83	*
PS2	Core (SP1/69)	Prince Albert	5.71	0.05	0.48	0.81	0.59	8	14	555	3.62	*
PS1	Core (SP1/69)	Prince Albert	7.35	0.04	0.48	0.46	1.04	7	6	579	3.84	*

Ro_c and Ro_m represents the calculated and measured vitrinite reflectance respectively, * indicates not analysed, and – depicts not determined.

Table 5 Geochemical parameters for describing kerogen type and hydrocarbon type generated (after Peters and Cassa, 1994)

Kerogen type	HI (mgHC/g TOC)	S2/S3 (mg)	Atomic H/C	Main expelled at peak maturity
I	> 600	> 15	> 1.5	Oil
II	300–600	10–15	1.2–1.5	Oil
II/III	200–300	5–10	1–1.2	Mixed oil and gas
III	50–200	1–5	0.7–1.0	Gas
IV	< 50	< 1.0	< 0.7	Dry Gas

Table 6 Organic carbon richness based on TOC data (after Peters, 1986)

Quality	TOC (wt%)	S_1 (mg)	S_2 (mg)
Poor	0–0.5	0–0.5	0–2.5
Fair	0.5–1.0	0.5–1.0	2.5–5
Good	1.0–2.0	1.0–2.0	5–10
Very good	> 2.0	> 2.0	> 10

kerogens, which are capable of generating both oil and gas at suitable burial depths (Figs. 6–7). The cross plots of S2 versus TOC, and HI against OI (Figs. 8–11) shows that the samples are mostly Type III kerogen (mainly derived from higher plants) and are expected to produce gas when matured. Generally, these results are comparable with the findings from Faure and Cole (1999) and Geel et al. (2013, 2015), where the lower Ecca Group formations were found to have Type-II/III, III and IV kerogens.

4.3 Thermal maturity level

The effects of deep burial on organic matter are irreversible and the highest P-T conditions are preserved after sedimentary sequences are exhumed. Thus, maturity indicators in organic matter are essential in assessing the level of thermal maturity. During pyrolysis, the obtained maximum temperature (Tmax) signifies the thermal energy required to break the most abundant chemical bonds in kerogen, which are associated with the generation of hydrocarbons (Mahlsterdt and Horsfield, 2012). The production of these hydrocarbons is related to the amount of hydrogen that is present in the rock and consequently, to its level of maturation (Nuñez-Betelu and Baceta, 1994). This is due to the fact that, the more mature the rock is, the lower the amount of hydrogen it contains and the higher amount of energy required to liberate the hydrocarbons. Peters and Cassa (1994) documented that Tmax values of less than 435ºC indicate immaturity of samples; Tmax values between 435ºC and 470ºC reflect maturity; and Tmax values above 470ºC represent over-maturity of the source rock. In this study, the thermal maturation level was estimated from the Tmax, vitrinite reflectance and production index (PI), at least where the TOC reached the minimum threshold of 0.5 wt% expected for clastic source rocks (Hunt, 1979; Hedberg and Moody, 1979). In addition, thermally mature sediments are thought to have Tmax values of ≥ 430ºC, with vitrinite reflectance (VR) values ranging between 0.6% and 1.3% (Peters and Cassa, 1994). Based on the aforementioned parameters,

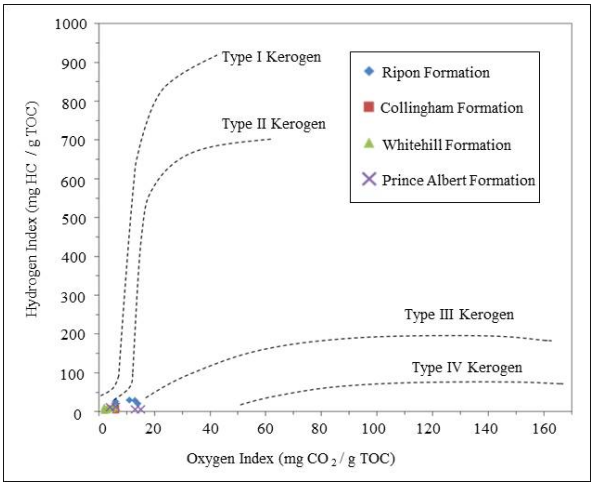

Fig. 6. Modified van Krevelen diagram of hydrogen index (HI) versus oxygen index (OI) for the Ecca shales in borehole KWV1, showing kerogen type. Organic matter in the Ecca Group is most consistent with Type II and III Kerogen.

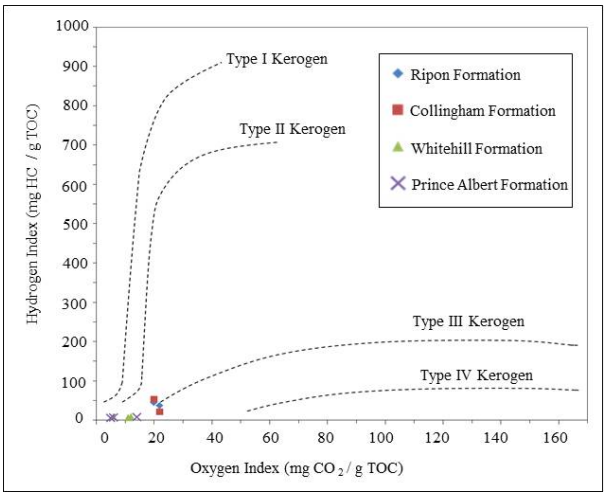

Fig. 7. Modified van Krevelen diagram of hydrogen index (HI) versus oxygen index (OI) for the Ecca shales in borehole SP1/69, showing kerogen type. Organic matter in the Ecca Group is most consistent with Type II and III Kerogen.

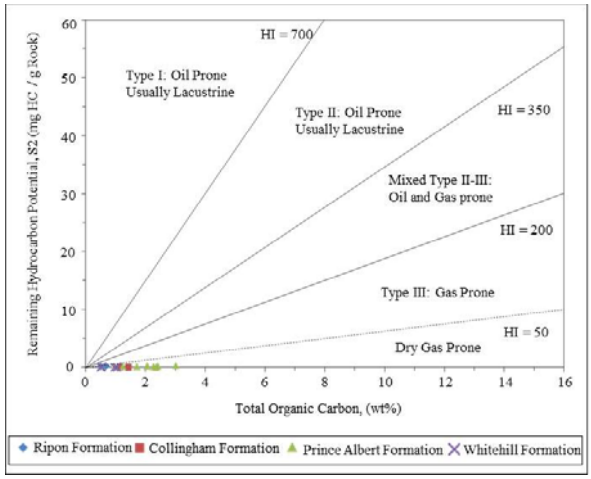

Fig. 8. Distribution of the analyzed samples into pyrolysis S2 versus total organic carbon (TOC) plot, showing kerogen quality of the Ecca shales in borehole KWV1. The plot indicates dry gas prone for the samples.

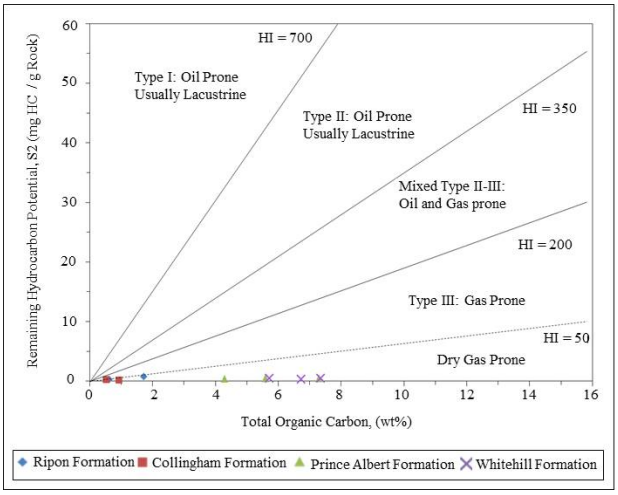

Fig. 9. Distribution of the analyzed samples into pyrolysis S2 versus total organic carbon (TOC) plot, showing kerogen quality of the Ecca shales in borehole SP1/69. The plot indicates dry gas prone for the samples.

contrasting levels of maturity were attained in the shales of the Ecca Group. In borehole KWV1 (Table 4; Fig. 12), the Tmax values vary between 415ºC and 429ºC, 318ºC and 411ºC in the Prince Albert and Whitehill Formations, respectively, indicating that the shales are immature. In contrast, the measured vitrinite reflectance (Rom) values for the Whitehill shales range between 2.22% and 3.69% indicating over-maturity. The overlying Ripon shales are over-matured, with Tmax values varying from 430ºC to 488ºC. At borehole SP1/69 (Table 4; Fig. 13), the Tmax values range between 555–590ºC, 524–601ºC, 513–599ºC, and 460–492ºC for the Prince Albert, Whitehill, Collingham and Ripon Formations, respectively. These values show that the shales are thermally over-mature, except for one sample from the Ripon Formation, which is marginally mature. In both boreholes, the Ecca shales are consistent with low HI values and relatively high Tmax values. The low HI values may reveal a high level of thermal maturity and/or higher proportions of reworked vitrinites in the shales. Generally, HI decreases at higher maturation levels as a result of the generated hydrocarbons, and this could also explain the low values of HI recorded at boreholes SP1/69 and KWV1. Perhaps, the organofacies of the lower Ecca formations show substantial contribution from terrestrial sources, as indicated on the HI/Tmax plots where most of the samples plot in the Type III kerogen field (Figs. 12–13).

In terms of vitrinite reflectance, the samples are generally vitrinite-lean; in fact, most samples do not

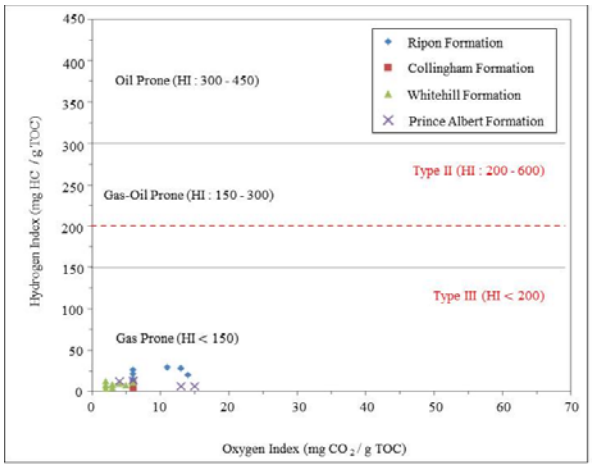

Fig. 10. Modified Van Krevelen diagram showing the organic matter types of the studied samples in borehole KWV1. The plot indicates gas prone for the samples.

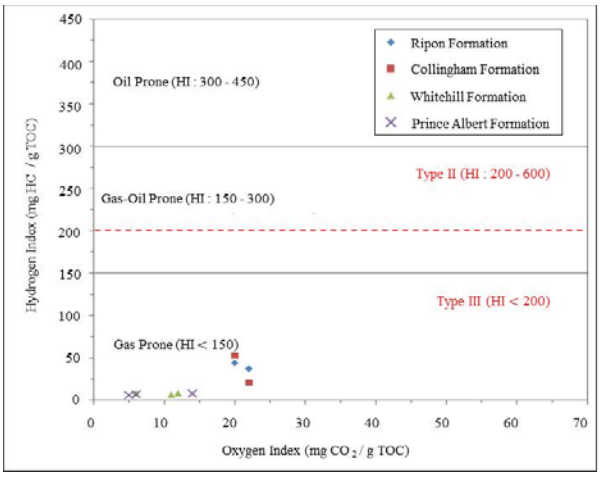

Fig. 11. Modified Van Krevelen diagram showing the organic matter types of the studied samples in borehole SP1/69. The plot indicates gas prone for the samples.

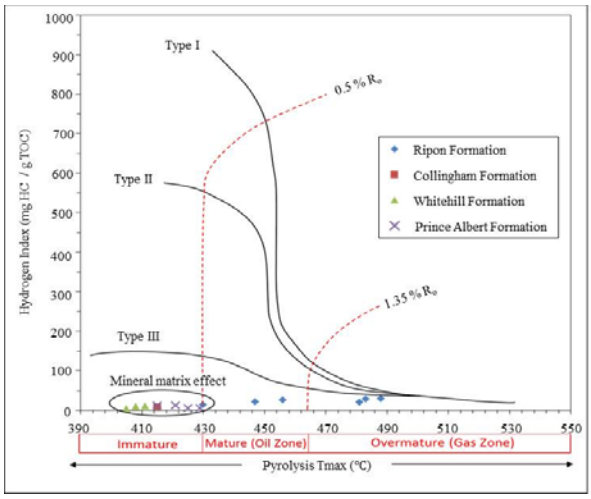

Fig. 12. Modified van Krevelen diagram of hydrogen index (HI) against Tmax of shale samples from the Prince Albert, Whitehill, Collingham and Ripon Formations in borehole KWV1, showing kerogen type and maturity.

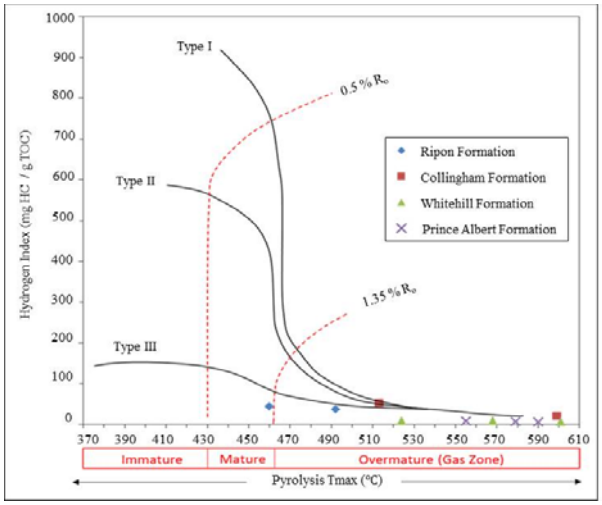

Fig. 13. Modified van Krevelen diagram of hydrogen index (HI) against Tmax of shale samples from the Prince Albert, Whitehill, Collingham and Ripon Formations in borehole SP1/69, showing kerogen type and maturity.

appear to contain vitrinite. Vitrinite particles were only determined in the Whitehill samples from borehole KWV1. A variety of solid bitumen, and possibly bituminite and inertinite fragments were observed in most samples (Figs. 14–17). Inertinite includes fusinite and inertodetrinite particles. Bituminite is a amorphous primary liptinite (ASTM, 2014). Solid bitumen is a secondary maceral generated from kerogen, and can be difficult to distinguish from vitrinite. By definition, solid hydrocarbons indicate hydrocarbon generation and migration in petroleum systems as a result of thermal conversion of kerogen, detected in shales and siltstones/sandstones that are mature and post-mature. Its absence would indicate thermal immaturity or lack of generative potential in the host rocks, or extreme maturity (average of > 5% *R*o). Figures 14–17 show images taken from four samples, providing an idea of changes in organic matter through the stratigraphy. The Prince Albert Formation is the basal formation of the Ecca Group. It consists predominantly of mudrocks (shale, mudstones and minor siltstones). The Prince Albert shales are thin bedded or well laminated and shows pencil cleavage (Fig. 14a). The Whitehill Formation disconformably overlies the Prince Albert Formation and is mainly made up of thin bedded, laminated, grayish-black carbonaceous shale with subordinate black chert lenses and mudstones (Fig. 15a). The black chert is more resistant to weathering and darker in color than the black carbonaceous shale. The black

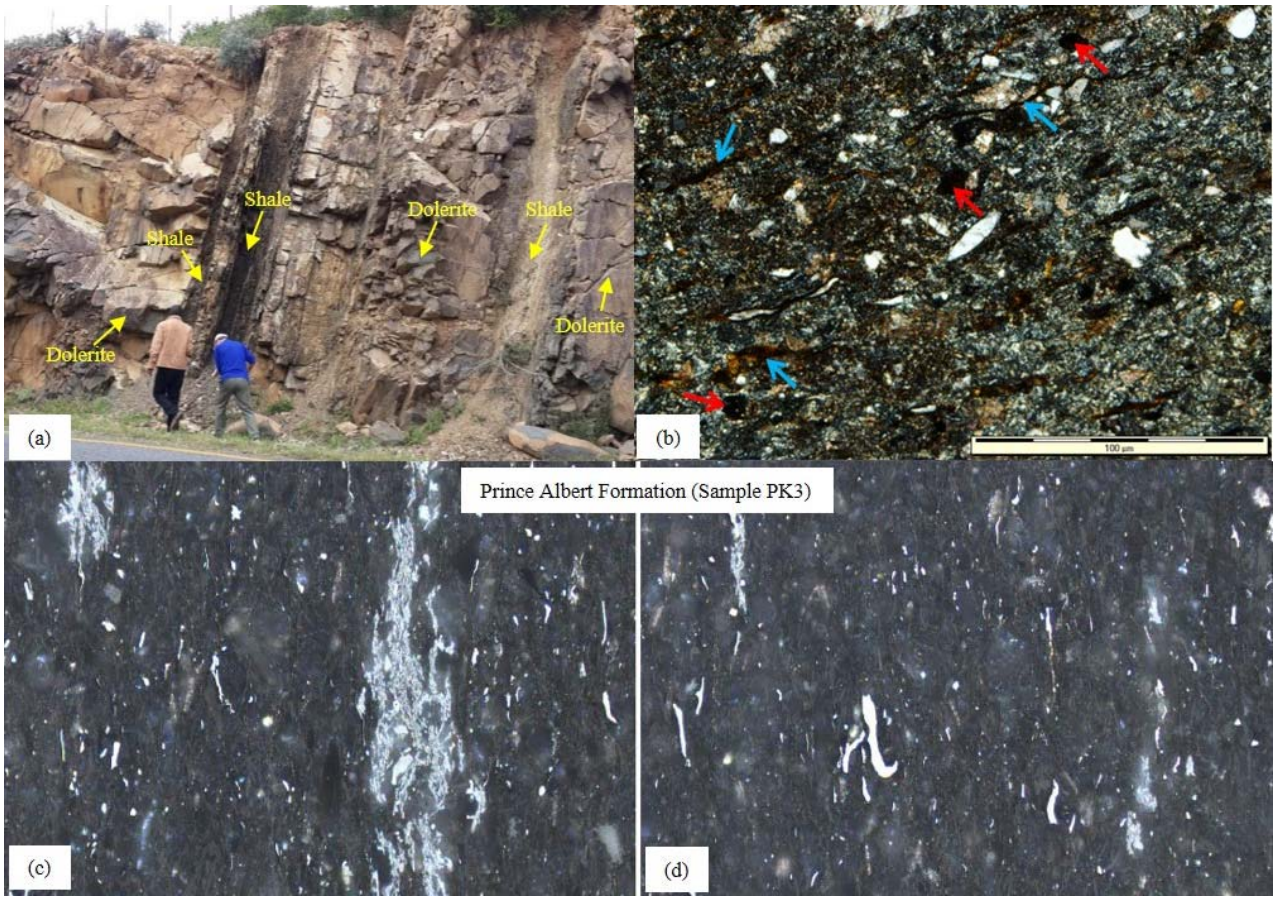

Fig. 14. (a), Photograph showing intrusions of dolerite in the dark-gray shale of the Prince Albert Formation along National road N2 between Grahamstown and Peddie; (b), thin-section photomicrograph of mudrock from the Prince Albert Formation showing siltstone with pyrite (dark area, red arrows) and hematite staining (blue arrow); (c–d), dispersed organic matter assessment of the Prince Albert shales, with colour images on the left (Fig. 14c) and monochromatic images on the right (Fig. 14d) showing fine mudstone, rare inertinite fragments with unusual white mineral inclusions, but no vitrinite.

shale is undergoing weathering to give a gray-whitish shale. The Collingham Formation conformably overlies the Whitehill Formation and is mainly made up of thin beds of dark grayish or dark greenish shales and very thin beds of weaker or softer yellowish claystones, which that are assumed to be ash-fall tuffs that had been altered to K-bentonite. The alternating layer structure depicts a classic rhythmite rock characteristic, which might be an indication that the deposits were possible turbiditic sediments. The claystones and mudstones constitute multiple cyclotherms of repeated units or couplets, termed rhythmites (Fig. 16a). The Ripon Formation conformably overlies the Collingham Formation and consists of sandstones alternating with mudstones (Fig. 17a). Silicification is well-developed in the Ripon Formation than in the Prince Albert, Whitehill and Collingham Formations. It is clear from the images that not all horizons actually contained organic matter beyond a few inertinite fragments. The TOC value possibly represents the carbonates rather than organic matter in most of the samples. Only samples from the Whitehill Formation contained appropriate organic matter on which to obtain reflectance data. The mean reflectance readings (%*R*o) indicate that the samples are over-mature, with readings ranging between 2–4 %*R*o. Furthermore, with the exception of one sample from the Ripon Formation, all others have calculated Ro_c values that are > 1.35%, indicating over-maturity of the samples.

The binary plot of Tmax versus production index (PI) can also be used as thermal maturity indicators (Figs. 18, 19). In borehole KWV1, the Ecca source rocks have pyrolysis Tmax and PI in the range of 318–488ºC and 0.16–0.57, respectively, indicating that most of the rocks are thermally immature (Fig. 18). Conversely, in borehole SP1/69, the source rocks have pyrolysis Tmax and PI values varying between 460–599ºC and 0.04–0.13, respectively, signifying that most of the shales are thermally over-matured and can only generate little or no hydrocarbon generation (inert carbon) (Fig. 19). The Tmax and PI values are partially in agreement with the

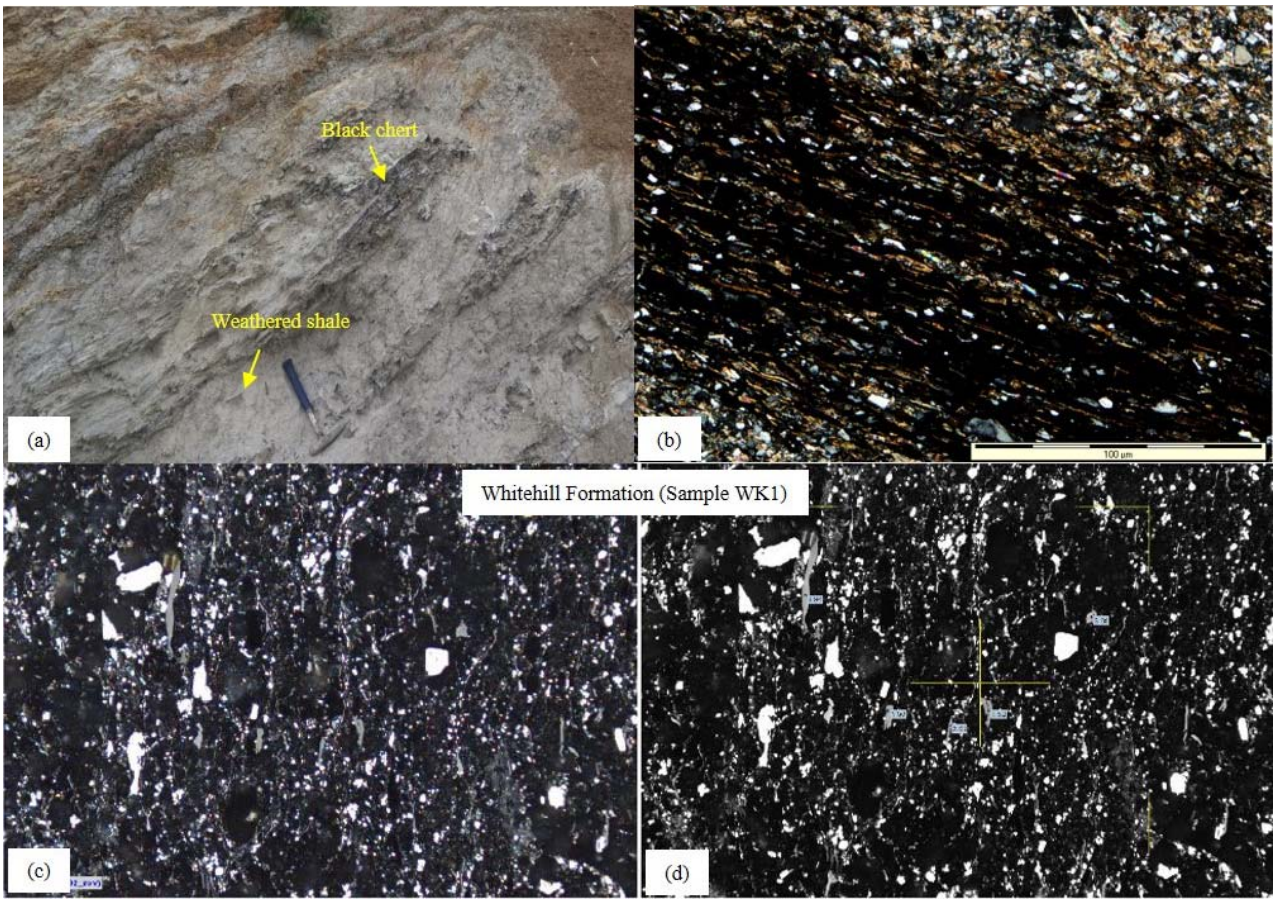

Fig. 15. (a), Photograph showing weathered thinly laminated carbonaceous shale with subordinate layers or lenses of black chert at the lower part of the Whitehill Formation along Regional road R67 between Grahamstown and Fort Beaufort (Ecca Pass). The black carbonaceous shale has been weathered to gray-whitish shale; (b), thin-section photomicrograph of carbonaceous siltstone of the Whitehill Formation showing mineral grains lying parallel to the lamination planes; (c–d), dispersed organic matter assessment of the Whitehill shales, with colour images on the left (Fig. 15c) and monochromatic images on the right (Fig. 15d) showing very fine-grained mudstone, more organic matter than samples from other formations, also confirmed by higher TOC. Lots of small, finely disseminated pyrite; blobs of solid bitumen, clear differentiation between organic matter–inertinite and vitrinite, rare evidence of possible devolatilisation in vitrinite-like particles.

vitrinite reflectance (%*R*o) values, indicating that the Ecca source rocks have entered the mature to late-mature gas window and are considered to be an effective source rock in the Main Karoo Basin of South Africa.

4.4 Hydrocarbon generation potential

TOC content alone cannot be used to establish satisfactorily the presence of potential and/or effective petroleum source rocks. This is due to the fact that different types of organic matter have different hydrocarbon yields for the same organic carbon content (Katz, 2006). Hence, a more direct measure of source rock hydrocarbon generative potential is required for detailed assessment. Tissot and Welte (1984) proposed a genetic potential (SP=S1+S2; see Table 1 for explanation) for the classification of source rocks. According to their classification scheme, rocks having SP of less than 2 mg HC/g rock are gas-prone, rocks with SP between 2 and 6 mg HC/g rock are oil-gas prone, and those with SP greater than 6 mg HC/g rock are good source rocks for oil. In borehole KWV1 (Fig. 20), SP values vary between 0.10–0.12 mg HC/g rock, 0.09–0.46 mg HC/g rock and 0.11–0.31 mg HC/g rock in the Prince Albert, Whitehill and Ripon shales, respectively. On the other hand, in borehole SP 1/69 (Fig. 21) where TOCs are relatively high (0.33–7.42 wt%), SP values vary between 0.42–0.53 mg HC/g rock in the Prince Albert Formation, 0.38–0.51 mg HC/g rock in the Whitehill Formation, 0.21–0.30 mg HC/g rock in the Collingham Formation and 0.24–0.8 mg HC/g rock in the Ripon Formation. These values in both boreholes are less than 2 mg HC/g rock, indicating gas-prone rocks.

In borehole KWV1, the binary plots of PI versus Tmax (Fig. 22) and S2/S3 against TOC ()Fig. 24 indicate that the Ecca rocks have potential to generate oil and gas. However, in borehole SP1/69, the plots of PI against Tmax (Fig. 23) and S2/S3 versus TOC (Fig. 25) show that

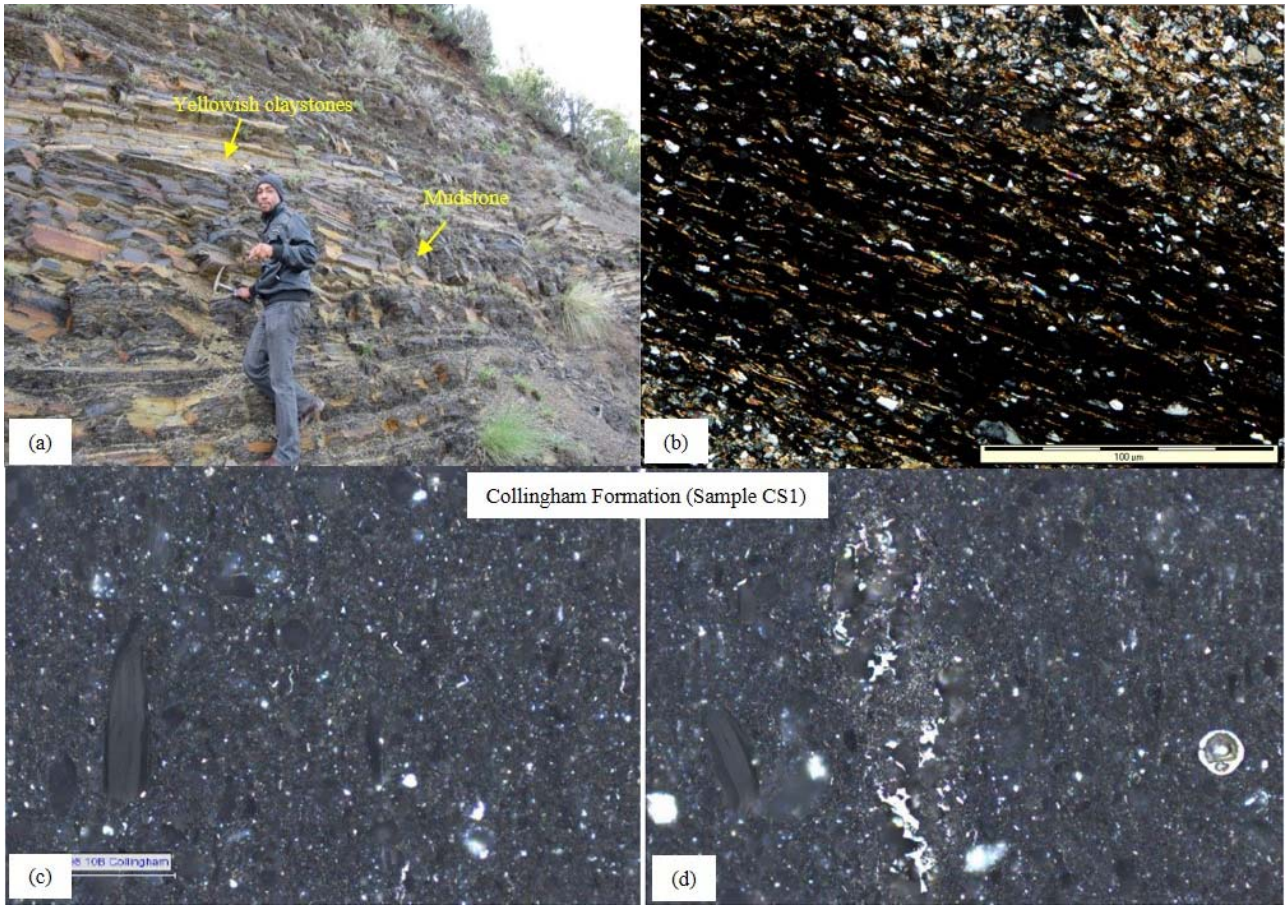

Fig. 16. (a), Photograph showing thinly bedded blackish mudstone of the Collingham Formation along Regional road R67 (Ecca Pass), interlayered with yellowish claystones, which are assumed to be ash-fall tuffs that have been altered to K-bentonite; (b), thin-section photomicrograph of mudrock showing manganese-iron-rich nodules in mudrock of the Collingham Formation; (c–d), dispersed organic matter assessment of the Collingham shales, with color images on the left (Fig. 16c) and monochromatic images on the right (Fig. 16d) showing very fine mudstone with quartz inclusions; no vitrinite determined, fluorescing component possibly carbonate minerals, rare inertinite particle, possible solid bitumen occurrence.

the rocks are mostly of Type III kerogen with fair to good potential of generating dry gas and minor condensate (wet gas). Likewise, the plot of HI against TOC revealed that the Ecca rocks are fair to excellent gas-oil source rocks (Figs. 26–29). A comparison of the similarities in the yield of hydrocarbons in the data set indicates that the carbonaceous shales of the Whitehill Formation have the highest yield in both boreholes. Burwood et al. (1995) reported that effective primary source rocks have S2 value of greater than 5 mgHC/g rock and effective non-source rocks (ENS) have S2 value of less than 1 mgHC/g rock. The S2 values for the analyzed samples are less than 1 mg HC/g rock, indicating both secondary source field and effective non-source rocks (ENS) (Figs. 30, 31). The plot of S1 versus TOC can be used to discriminate between non-indigenous (allochthonous) and indigenous hydrocarbons (autochthonous). This relationship (Figs. 32, 33) shows that the studied Ecca rocks are characterized by autochthonous hydrocarbons.

5 Comparison of Reservoir Characteristics

As documented by Chere (2015), the potential of shale gas in a sedimentary basin mainly depends on the structural and thermal history of the basin. Basins that have experienced major folding and faulting may not retain hydrocarbons due to thermo-tectonic driven migration (Chere, 2015). Hydrocarbons within deeply buried basins may only have potential for dry gas since they are subjected to high temperatures and pressures. Reservoir characteristics of the Ecca shales in the study area are compared to the Whitehill Formation in Jansenville (Geel et al., 2013, 2015; Chere, 2015) as well as to the Marcellus and Barnett Shales in the United States (Bruner and Smosna, 2011). The area investigated is located close to the CFB and is intruded by dolerites, whereas the Marcellus and Barnett Shales are structurally inconstant. Exploitable gas-bearing shales generally have reservoir characteristics that include high organic richness,

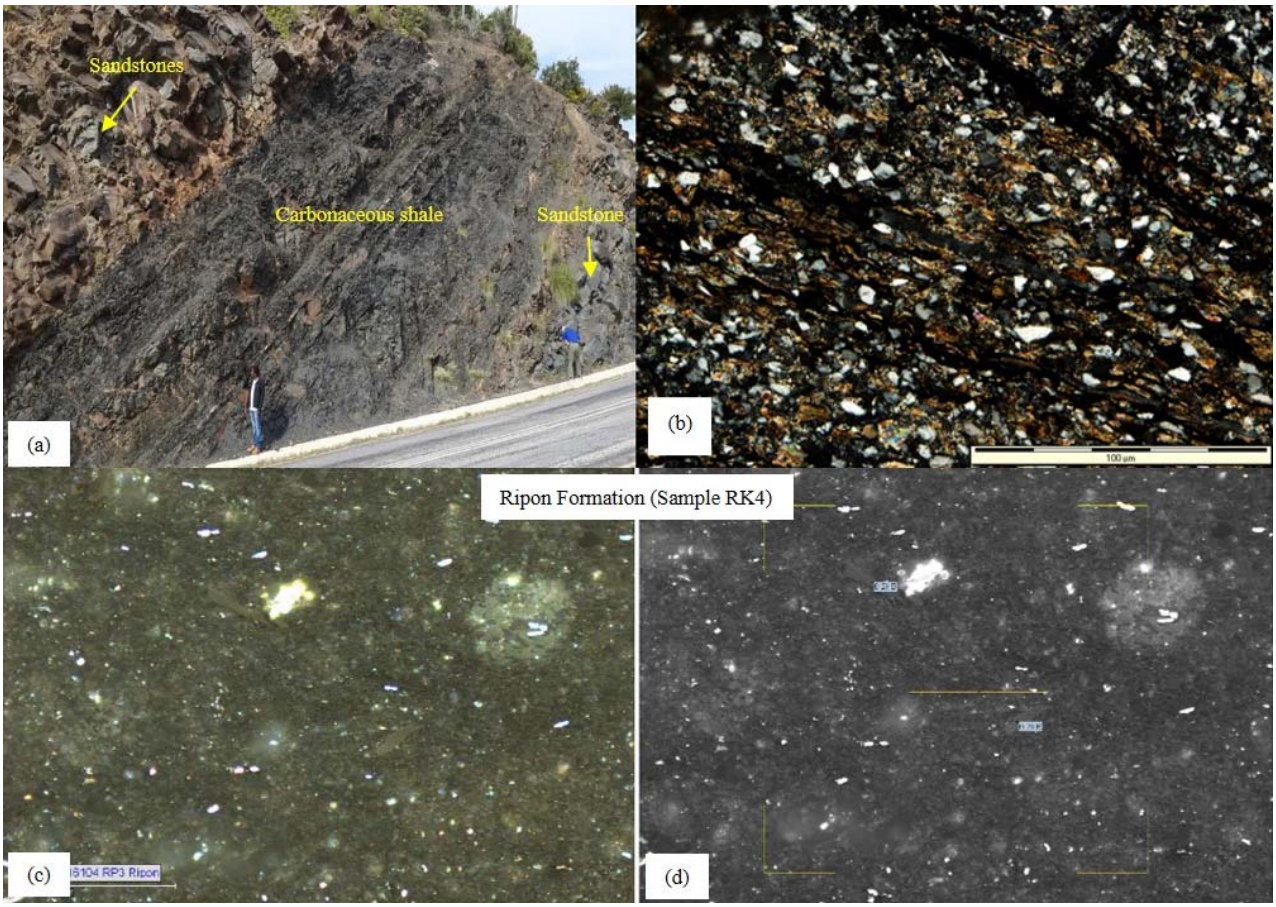

Fig. 17. (a), Photograph showing dark gray greywacke and grayish-black carbonaceous shale in the Upper Member of the Ripon Formation along Regional road R67 (Ecca Pass); (b), thin-section photomicrograph of carbonaceous siltstone of the Ripon Formation showing mineral grains lying parallel to the lamination planes; (c–d), dispersed organic matter assessment of the Ripon shales, with colour images on the left (Fig. 17c) and monochromatic images on the right (Fig. 17d) showing very fine-grained mudstone with carbonate inclusions; no vitrinite and fluorescence determined and very rare inertinite fragments.

thermally mature, high porosity resulting from decomposition of organic matter, and mineral-induced brittleness. Mineralogy of shale from the Whitehill Formation suggests suitable brittleness due to high quartz, calcite and dolomite content. Several studies including those of Kuuskraa et al. (2011), Geel et al. (2013, 2015) and Chere (2015) show that the Whitehill Formation complies with most of the aforementioned characteristics and therefore is the main target for unconventional shale gas exploration in the southern Main Karoo Basin. Reservoir characteristics, i.e. carbon content, lateral extent, thickness, porosity and permeability, of the Whitehill Formation as a suitable shale gas host, obtained in this study as well as those of Geel et al. (2013, 2015) and Chere (2015) compare favourably with the Marcellus and Barnett shales, which are currently exploited for gas in the United States (Bruner and Smosna, 2011; Hoelke, 2011). For instance, on average, the measured TOC value for the carbonaceous black shale of the Whitehill Formation is slightly higher than the average TOC value for the Barnett Shale (Table 7). Furthermore, the measured vitrinite reflectance values reach maximum values of about 3.5 %*R*o, which is the same with those measured in the Barnett Shale and comparable with the result of Geel et al. (2013) and Chere (2015). This perhaps indicates that the Whitehill Formation has potential for being a profitable shale gas resource, especially in areas or locations where the shales are not intruded by dolerites and are far away from the CFB. This is because dolerite intrusions as well as proximity to CFB in combination with depth of burial may have destroyed or over-cooked the organic matter that is present in the rock. The characteristics of shales from the Whitehill Formation (Table 7) show that they have the potential for holding significant amounts of gas and are frackable (high quartz content and low/absence of smectite). Generally, it can be said that the Whitehill Formation is comparable to the Barnett and Marcellus Shales.

Decker and Marot (2012) noted that the Collingham Formation should also be considered for shale gas

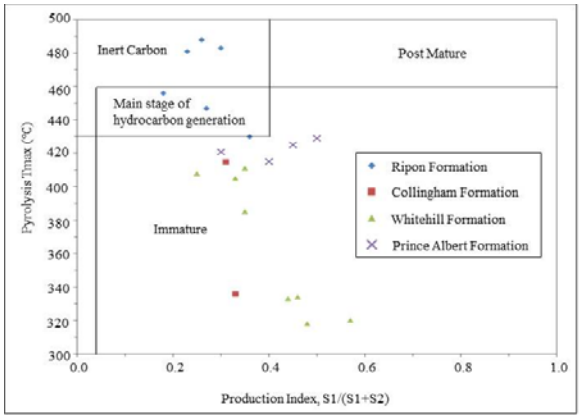

Fig. 18. Plot of pyrolysis Tmax versus production index (PI), showing the maturation and nature of the hydrocarbon products of the Ecca source rocks in borehole KWV1.

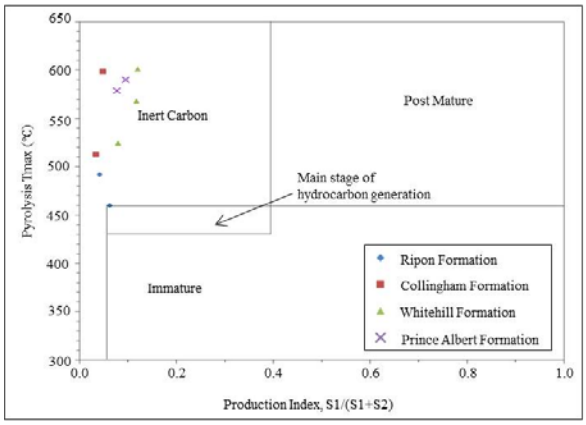

Fig. 19. Plot of pyrolysis Tmax versus production index (PI), showing the maturation and nature of the hydrocarbon products of the Ecca source rocks in borehole SP1/69.

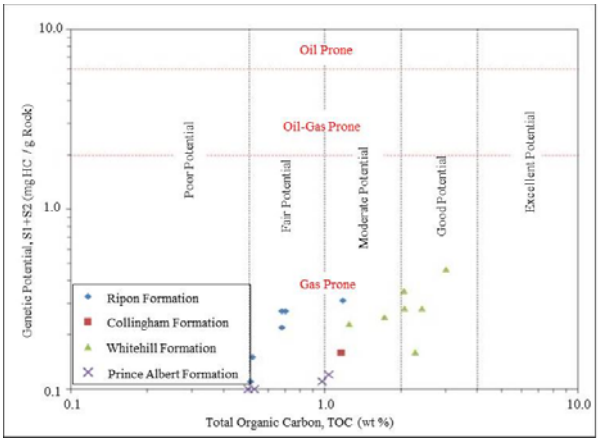

Fig. 20. Binary plot of genetic potential versus TOC for the Ecca shales in borehole KWV1 showing source rock generative potential (after Maravelis and Zelilidis 2010).

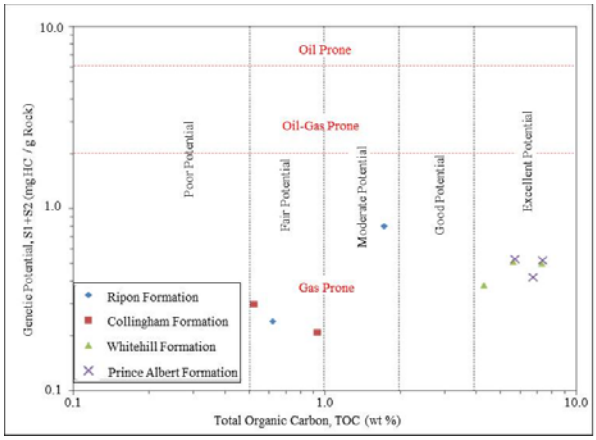

Fig. 21. Binary plot of genetic potential versus TOC for the Ecca shales in borehole KWV1 showing generative source rock potential (after Maravelis and Zelilidis 2010).

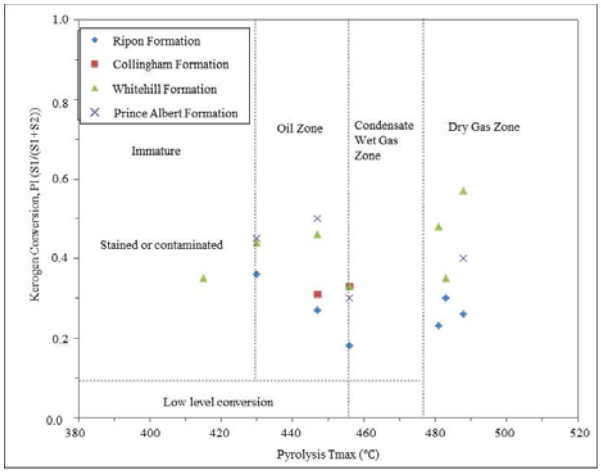

Fig. 22. Plot of production index (PI) versus Tmax showing hydrocarbon production for the Ecca source rocks in borehole KWV1.

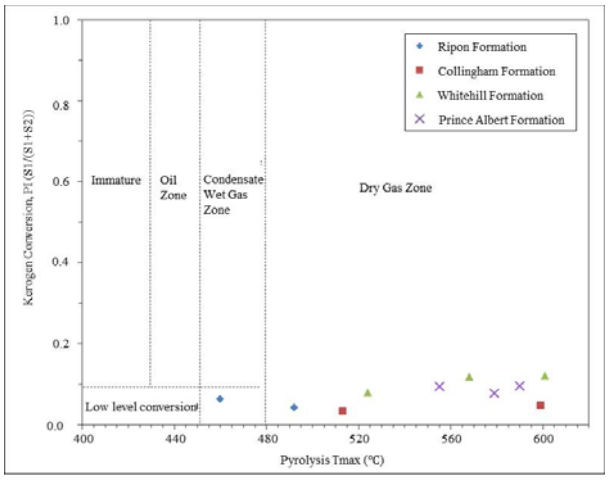

Fig. 23. Plot of production index (PI) versus Tmax showing hydrocarbon production for the Ecca source rocks in borehole SP1/69.

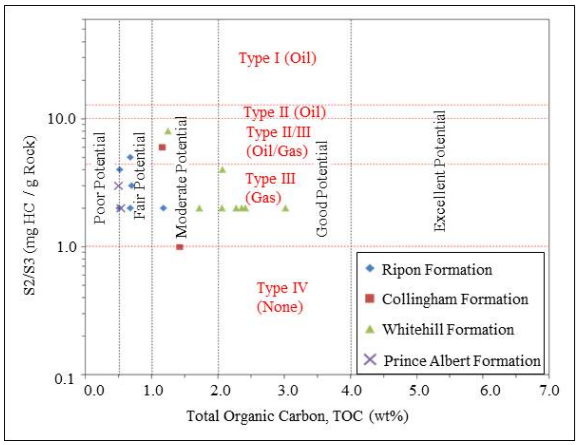

Fig. 24. Binary plot of S2/S3 versus total organic carbon (TOC) showing generative source rock potential for the Ecca Group in borehole KWV1.

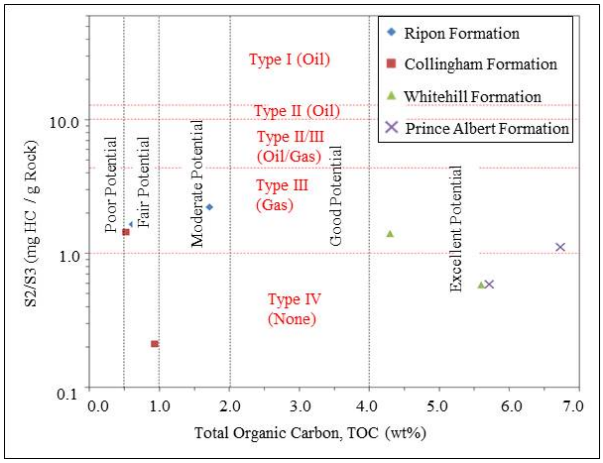

Fig. 25. Binary plot of S2/S3 versus total organic carbon (TOC) showing generative source rock potential for the Ecca Group in borehole SP1/69.

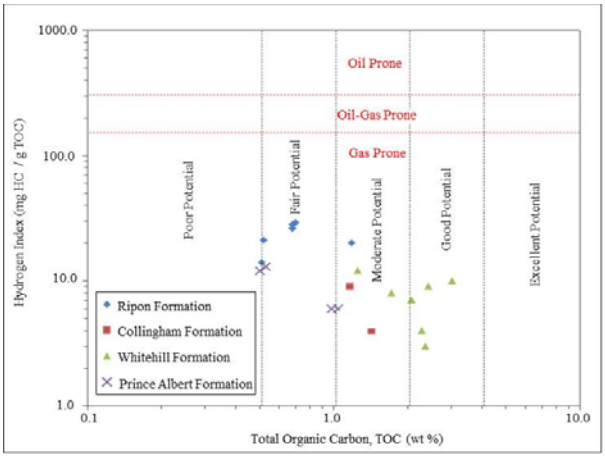

Fig. 26. Binary plot of hydrogen index (HI) against TOC for the Ecca shales in borehole KWV1 showing generative source rock potential (after Maravelis and Zelilidis 2010).

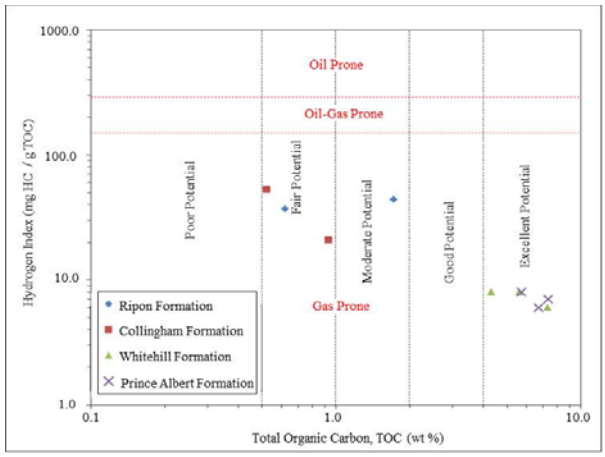

Fig. 27. Binary plot of hydrogen index (HI) against TOC for the Ecca shales in borehole SP1/69 showing generative source rock potential (after Maravelis and Zelilidis 2010).

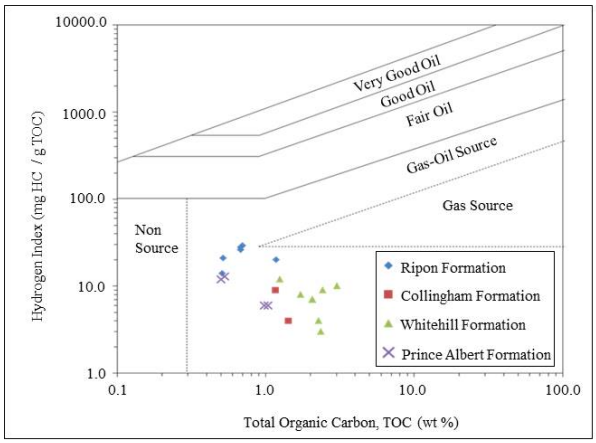

Fig. 28. Binary plot of HI versus total organic carbon (TOC) showing source rock richness for the Ecca Group in borehole KWV1.

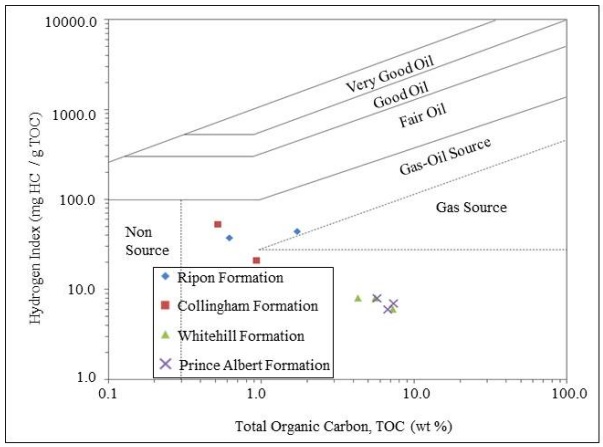

Fig. 29. Binary plot of HI versus total organic carbon (TOC) showing source rock richness for the Ecca Group in borehole SP1/69.

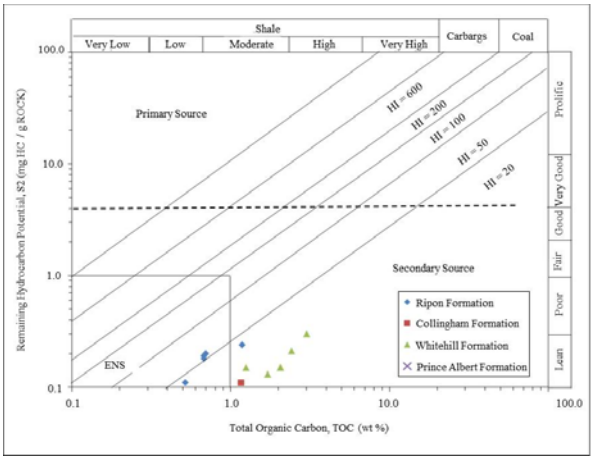

Fig. 30. S2 versus TOC plot for source rock quality of the Ecca shales in borehole KWV1; primary source field is ascribed to sediments with S2 greater than 5 kg/ton rock; ENS refers to effective non-source field (after Burwood et al. 1995).

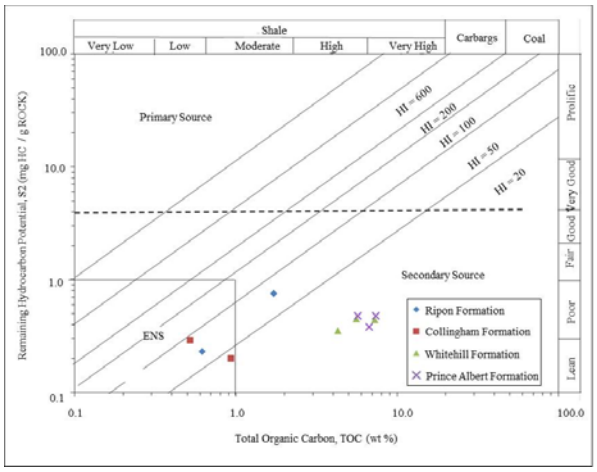

Fig. 31. S2 versus TOC plot for source rock quality of the Ecca shales in borehole SP1/69. Note: Primary source field is ascribed to rocks with S2 greater than 5 kg/ton rock; ENS refers to effective non-source field (after Burwood et al. 1995).

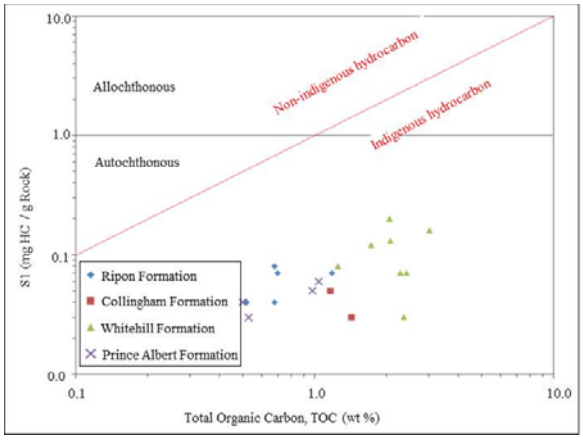

Fig. 32. Binary plot of S1 against TOC for the Ecca shales showing generated indigenous–non indigenous hydrocarbon in borehole KWV1 (after Maravelis and Zelilidis 2010).

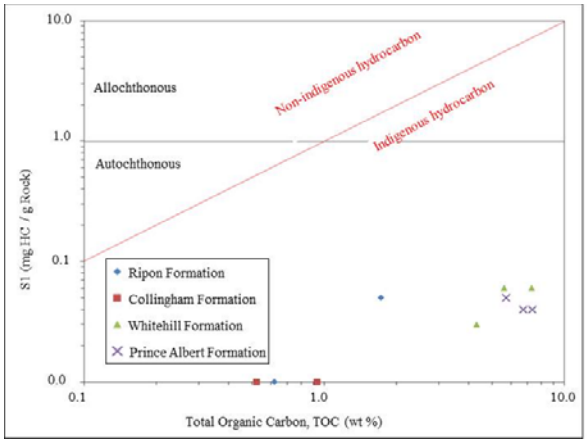

Fig. 33. Binary plot of S1 against TOC for the Ecca shales showing generated indigenous–non indigenous hydrocarbon in borehole SP1/69 (after Maravelis and Zelilidis 2010).

exploration, only if TOC values were found constantly to exceed 3% over large areas of the basin. In this study, the measured TOC values for the Collingham Formation range from 0.22 to 0.93%, which compares well with the TOC values obtained by Geel et al. (2013) and Black et al. (2016). In addition, the shales have an average porosity and permeability values of 0.39% and 0.02 mD, respectively, which is much lower than that measured in the Whitehill Formation as well as those determined for active shale gas plays in the United States (Table 7). The combination of low carbon content, very low porosity and permeability values as well as the laminated nature of the strata shows that the Collingham Formation would be a poor source rock for gas, but an effective seal to the underlying potentially gas-bearing Whitehill Formation. The overlying carbonaceous shale of the Ripon Formation has an average TOC, porosity and permeability of 2.62%, 0.60% and 0.05 mD, respectively. This unit could also be a good hydrocarbon reservoir due to their closeness to the organic-rich Whitehill Formation. Furthermore, the formation contains laterally extensive thick sandstone units intercalating or capping the carbonaceous shales. These features are usually associated with an ideal hydrocarbon reservoir as long as the 'poroperm' values are conducive to hydrocarbon storage. In terms of the measured porosity and permeability values, the Ripon Formation is comparable to those of Campbell (2014) but not comparable with the globally productive sandstones of the Marnoso Arenacea Formation, UK, and Foinaven Field, USA (Table 8). For instance, the currently producing Foinaven Field has porosity values that are about 30 times higher than that of the Ripon Formation, allowing for the effective storage of hydrocarbons (Campbell, 2014). The potential pore spaces in the Ripon

Table 7 Comparison of reservoir characteristics of the Whitehill Shale to those of the Marcellus and Barnett Shales (modified from Chere, 2015)

Property		Whitehill (Permian Ecca shale, Karoo Basin, RSA) (**This study**)	Whitehill (Permian Ecca shale, Karoo Basin, RSA) (Geel et al., 2013, 2015)	Whitehill (Permian Ecca shale, Karoo Basin, RSA) (Chere, 2015)	Marcellus (Devonian Shale, Appalachian Basin USA) (Bruner and Smosna, 2011)	Barnett (Mississippian shale Fort Worth Basin, USA) (Bruner and Smosna, 2011; Hoelke, 2011)
Lithology		Organic rich black shale	Organic rich, pyritic black shale	Organic rich, pyritic black shale	Organic rich black shale	Organic rich black shale
Mineralogy (%)	Quartz	20–42	13–55	32–42	10–60	35–50
	Clays (illite)	4–26	5–29		10–35	10–50
	Calcite, sericite dolomite	2–38	3–62		3–50	0–30
	Feldspars	0–28	0–24		0–4	7
	Pyrite	2–12	1–16		5–13	5
	Phosphate, gypsum	trace	trace		trace	trace
	Mica	0–3	3–22		5–30	0
TOC (wt%)		0.5–7.3	0.7–8.15	1.6–7.3	1–10	2–6
Tmax (°C)		318–601	≥563	290–601	≥475	≥455
Vitrinite reflectance (% *R*o)		2.2–3.5	4	2–3.6	0.7–3.5	0.6–1.9
Kerogen Type		Mixture of type II/III, III	Mixture of type II and III	Mixture of type I/II, Type III, Type IV	type II and III	Mostly type II
Porosity (%)		1–5.5	2.9		3–6	3–6
Average permeability (mD)		0.89			-	-
Thickness (m)		18–46	≈ 28	≈ 30–60	15	Max. 304; Av. 31
Estimated potential yield		-	-	-	50–900	2.5bcf-40tcf

Formation sandstones are filled by smaller particles (i.e. clay minerals) and organic matter, thus reducing the potential hydrocarbon storage volume of the sandstone. Again, the permeability of the Ripon Formation is very low as compared to the Foinaven Field, thus preventing migration of potential hydrocarbons.

6 Conclusions

The organic geochemical investigation of shale samples from the Ecca Group indicates the presence of gas-prone potential source rocks with fair to excellent source generative potential. Specifically, the shales of the Prince Albert Formation are fair to good, while the carbonaceous shales of the Whitehill Formation are good to excellent. The Ecca source rocks have TOC values ranging from 0.11 to 7.35 wt%. Generally, the average TOC values of the shales in borehole SP1/69 (depth between 3400–3720 m) are higher than those in KWV1 (depth between 1300–2450 m), suggesting that the hydrocarbon potential for the Ecca lithofacies in the East London area is better than in the Butterworth area.

The Ecca shales are consistent with low HI values and relatively high Tmax values. The low HI values possibly indicate a high level of thermal maturity and/or higher proportions of reworked vitrinites in the shales. The over-maturity of the shale may be due to the proximity of the study area to the CFB. Also, excessive burial might have resulted in the loss of potential hydrocarbons (depths greater than 2500 m and 3800 for KWV1 and SP1/69, respectively). Reservoirs compartmentalization as well as the burning off of hydrocarbons as a result of numerous dolerite intrusions might also have resulted in additional loss of potential hydrocarbons. The binary plots of HI against OI, and HI versus Tmax shows that the Ecca shales are of Type II and mixed Type II–III kerogen, which are capable of generating both gas and minor oil at suitable burial depth. The bulk of the organic matter appeared to be either Type II or mixed Types II/III, i.e. marine–terrestrial input. There is a possibility that during deposition, the southeastern Karoo region was closer to a shelf, enabling terrestrial input, whereas the marine signature is potentially derived from short lived marine transgressions.

Table 8 Comparison of reservoir potential of the carbonaceous shale and sandstones of the Ripon Formation, Ecca Group (South Africa) with those of the Marnoso Arenacea Formation (United Kingdom) and the Foinaven Field (United States) (modified from Campbell, 2014)

Property	Ripon (Permian Ecca sandstone) (**This Study**)	Ripon (Permian Ecca sandstone) (Campbell, 2014)	Marnoso Arenacea Formation, (Northern Italy) Amy et al., 2009)	Foinaven Field (Palaeocene sandstone, Off-shore, Scotland) (Huggins, 2007)
Lithology	Fine grained sandstones intercalated with shale	Medium to fine grained sandstone	Sandstone and mudstone	Fine to medium grained sandstone
Porosity (%)	0.38–0.84	1	0.15	23–30
Permeability	0.001–0.992	0.045	100	500–2000

The S2 values for the analyzed samples are less than 1 mgHC/g rock, indicating a secondary source field. The plot of S1 versus TOC shows that the source rocks were characterized by autochthonous hydrocarbons. Based on the geochemical data, the shales of the Whitehill Formation are earmarked as a potential hydrocarbon source rock and it can be further inferred that these rocks are in immature to over-mature states and have potential of producing gas in the present-day. Generally, the Whitehill Formation is comparable to the Marcellus and Barnett Shales. This further supports the assumption that the Whitehill Formation could be a potential and profitable shale gas play, but only when explored in a dolerite-free area and relatively far away from the CFB.

Acknowledgements

The authors would like to thank the DST-NRF Centre of Excellence for Integrated Mineral and Energy Resource Analysis (CIMERA) and the Govan Mbeki Research and Development Centre (GMRDC) at Fort Hare University for financial support.

Manuscript received Aug. 21, 2017
accepted Apr. 5, 2018
edited by Susan Turner and Fei Hongcai

References

Advance Resource International, 2013. *Shale gas and oil assessment in Karoo Basin, South Africa*. EIA/ARI World Shale Gas and Shale Oil Resource Assessment, EIA/ARI, Advanced Resources International, Arlington, USA, 1–14. Available online: https://www.eia.gov/analysis/studies/worldshalegas/pdf/South_Africa_2013.pdf

ASTM D7708-14, 2014. *Standard Test Method for Microscopical Determination of the Reflectance of Vitrinite Dispersed in Sedimentary Rocks*. West Conshohocken, PA*: American Society for Testing and Materials ASTM International,* 1–14.

Amy, L.A., Peachy, S.A., Gardiner, A.A., and Talling, P.J., 2009. Prediction of hydrocarbon recovery from turbidite sandstones with linked-debrite facies: Numerical flow simulation studies. *Marine and Petroleum Geology*, 26: 2032–2043.

Barker, C., 1996. *Thermal Modelling of Petroleum Generation: Theory and Applications*. New York: Elsevier, 1–62.

Bilgen, S., and Sarıkaya, İ., 2016. New horizon in energy: Shale gas. *Journal of Natural Gas Science and Engineering*, 35: 637–645.

Bipartisan Policy Center, 2012. *Shale gas: new opportunities, new challenges*. Washington, USA: Bipartisan Policy Center Energy Report, 1–26.

Black, D.E., Booth, P.W.K., and de Wit, M.J., 2016. Petrographic, geochemical and petro-physical analysis of the Collingham Formation near Jansenville, Eastern Cape, South Africa – potential cap rocks to shale gas in the Karoo. *South African Journal of Geology*, 119: 171–186.

Booth, P.W.K., and Goedhart, M.L., 2014. Thrust faulting in the northernmost foreland zone of the Cape Fold Belt, Fort Beaufort, Eastern Cape. South Africa. *South African Journal of Geology*, 117: 301–315.

Branch, T., Ritter, O., Weckman, U., Sachsenhofer, R., and Schilling, F., 2007. The Whitehill Formation- a high conductivity marker horizon in the Karoo Basin. *South African Journal of Geology*, 110: 465–476.

Bruner, K.R., and Smosna, R.A., 2011. *A Comparative Study of the Mississippian Barnett Shale, Fort Worth Basin and Devonian Marcellus Shale, Appalachian Basin*. U.S. Department Energy, National Energy Technology Laboratory, DOE/NETL/2011/1478, 106pp.

Burwood, R., De Witte, S.M., Mycke, B., and Paulet, J., 1995. Petroleum geochemical characterisation of the lower congo coastal basin bucomazi formation. In: Katz, B.J. (ed.), *Petroleum Source Rocks*. Berlin: Springer-Verlag, 235–263.

Business Day Live, 2014. South Africa petroleum agency's Karoo shale-gas estimate 'far lower'. *http://www.bdlive.co.za/business/energy/2014/02/21/sapetroleumagencys-karoo-shale-gas-estimate-far-lower.html*

Bustin M.R., Bustin A., Chamlmers G., Murthy V., Laxmi C., and Cui, X., 2009. Shale gas opportunities and challenges. Search and Discovery Article No. 40382, 18-27. Available online: *http://www.searchanddiscovery.com/pdfz/documents/2009/40382bustin/ndx_bustin.pdf.html*

Campbell, S.A., 2014. *The Ecca Type Section (Permian, South Africa): An outcrop analogue study of conventional and unconventional hydrocarbon reservoirs*. M.Sc. Dissertation. Rhodes University, South Africa, 1–105.

Catuneanu, O., Wopfner, H., Eriksson, P.G., Cairncross, B., Rubidge, B.S., Smith, R.M.H., and Hancox, P.J., 2005. The Karoo basins of south-central Africa. *Journal of African Earth Sciences*, 43: 211–253.

Chere, N., 2015. *Sedimentological and geochemical investigations on borehole cores of the Lower Ecca Group black shales, for their gas potential - Karoo Basin, South Africa*. M.Sc. Dissertation. Nelson Mandela Metropolitan University, South Africa, 1–268.

Chevallier, L., and Woodford, A.C., 1999. Morpho-tectonics and mechanism of emplacement of the dolerite rings and sills of the western Karoo, South Africa. *South African Journal of Geology*, 102: 43–54.

Chevallier, L., Goedhart, M., and Woodford, A.C., 2001. The influences of dolerite sill and ring complexes on the occurrence of groundwater in Karoo fractured aquifers: a morpho-tectonic approach. Cape Town, South Africa: *Water Research Commission Report*, 937/1/01, 1–146.

Cole, D.I., 1992. Evolution and Development of the Karoo Basin. In: De Wit, M.J. and Ransome, I.G.D., (eds.), *Inversion Tectonics of the Cape Fold Belt, Karoo and Cretaceous Basins of Southern Africa*. Rotterdam, The Netherlands: Balkema, 87–100.

Cole D.I., 2005. Prince Albert Formation. *Catalogue of South African Lithostratigraphic Units*. South Africa: *South African Committee for Stratigraphy*, p. 4.

Cook P., Beck V., Brereton D., Clark R., Fisher B., Kentish S., Toomey J., and Williams J., 2013. Engineering energy: unconventional gas production. *Report for the Australian Council of Learned Academies*, Melbourne: *ACOLA*, 1–251. www.acola.org.au.

Council of Canadian Academies, 2014. Environmental Impacts

of Shale Gas Extraction in Canada: The expert panel on harnessing science and technology to understand the environmental impacts of shale gas extraction. Ottawa (ON): Council of Canadian Academies,1–262.

Curtis, J.B., 2002. Fractured shale-gas systems. *American Association of Petroleum Geologists Bulletin*, 11: 1921–1938.

Decker, J., and Marot. J., 2012. *Annexure A: Resource Assessment. In: Department of Mineral Resources, 2012. Report on investigation of hydraulic fracturing in the Karoo Basin of South Africa*. pp, 81; p.15 annexures. Available at: http://www.dmr.gov.za/publications/viewdownload/182/854.html

De Wit, M.J., and Ransome, I.G., 1992. Regional inversion tectonics along the southern margin of Gondwana. In: De Wit, M.J., and Ransome, I.G. (eds.), *Inversion tectonics of the Cape Fold Belt, Karoo and Cretaceous Basins of Southern Africa*. Rotterdam, The Netherlands: Balkema, 15–22.

Duncan, R.A., Hooper, P.R., Rehacek, J., Marsh, J.S., and Duncan, A.R., 1997. The timing and duration of the Karoo igneous event, southern Gondwana. *Journal of Geophysical Research*, 102: 18127–18138.

Du Toit, J.C.O., and O'Connor, T.G., 2014. Changes in rainfall pattern in the eastern Karoo, South Africa, over the past 123 years. *Water South Africa*, 40: 453–460. Available at: https://www.ajol.info/index.php/wsa/article/view/105835/95842

Faure K., and Cole D., 1999. Geochemical evidence for lacustrine microbial blooms in the vas Permian Main Karoo, Parana, Falkland Islands and Huab basins of the southwestern Gondwana. *Palaeogeography, Palaeoclimatology, Palaeoecology*, 152: 189–213.

Ferreira, J.C., 2014. *Characterization of potential source rocks of the Prince Albert, Whitehill and Collingham formations in the Laingsburg sub-basin, South Africa*. M.Sc. Dissertation. University of Western Cape, South Africa, 1–115.

Fildani, A., Drinkwater, N. J., Weislogel, A., McHargue, T., Hodgson, D., and Flint, S., 2007. Age controls of the Tanqua and Laingsburg deep-water systems: new insights on the evolution and sedimentary fill of the Karoo basin, South Africa. *Journal of Sedimentary Research*, 77: 901–908.

Fildani, A., Weislogel, A., Drinkwater, N. J., McHargue, T., Tankard, A., Wooden, J., Hodgson, D., and Flint, S., 2009. U-Pb zircon ages from the southwestern Karoo Basin, South Africa - Implications for the Permian-Triassic boundary. *Geology*, 37: 719–722.

Geel, C., De Wit, M.J., Booth P.W.K., Schulz, H.M., and Horsfield, B., 2015. Palaeo-environment, diagenesis and characteristics of Permian Black Shales in the Lower Karoo Supergroup flanking the Cape Fold Belt near Jansenville, Eastern Cape, South Africa: Implications for shale gas potential of the Karoo Basin. *South African Journal of Geology*, 18, 249–274.

Geel, C., Schulz, H.M., Booth, P., De Wit, M., and Horsfield, B., 2013. Shale gas characteristics of Permian black shales in South Africa: results from recent drilling in the Ecca Group (Eastern Cape). *Energy Procedia*, 40: 256–265.

Hackett, D.P., Byrd, M.J., Davis, L.J., Sanders, D.B., and de Doe, D.R., 2012. Shale gas – environmental law and regulation. *Global Environment SG-ELR, Baker and McKenzie, U.S., 1–*9.

Hälbich, I.W., 1993. Global Geoscience Transect 9. The Cape Fold Belt - Agulhas Bank transect across Gondwana Suture, Southern Africa. *American Geophysical Union Special Publication*, 202: 1–18.

Hälbich, I.W., Fitch, F.J., and Miller, J.A., 1983. Dating the Cape orogeny. *Special Publications of the Geological Society of South Africa*, 12: 149–164.

Hansma, J., Eric, T. E., Jourdan, F., Schrank, C., and David A.D., 2015. The timing of the Cape Orogeny: New 40Ar/39Ar age constraints on deformation and cooling of the Cape Fold Belt, South Africa. *Gondwana Research*, 32: 122–137.

Hedberg, H.D., and Moody, J.O., 1979. Petroleum prospects of deep offshore. *American Association of Petroleum Geologists Bulletin*. 63: 286–300.

Hoelke, J.D., 2011. *Chemostratigraphy and Paleoceanography of the Mississippian Barnett Formation, Southern Fort Worth Basin, Texas, USA.* MSc Dissertation, University of Texas, Arlington, 1–96.

Horsfield, B., and Schulz, H.M., 2010. Shale Gas Research: the way forward for Europe. *Oilfield Technology*, 4: 14–18.

Huggins, P., 2007. Heterogeneity and flow barriers in turbidites, Foinaven Field, UKCS. In: *69th EAGE Conference and Exhibition* incorporating SPE EUROPEC 2007 at ExCel, LondonLondon, WO11 North Sea Core Workshop. Available at: http://www.earthdoc.org/publication/publicationdetails/?publication=7783

Hunt, J. M., 1979. *Petroleum Geochemistry and Geology*. San Francisco: Freeman and Company, 1–617.

Isbell, J.L., Cole, D.I., and Catuneanu, O., 2008. Carboniferous-Permian glaciation in the Main Karoo Basin, South Africa: Stratigraphic, depositional controls and glacial dynamics. In: C.R. Fielding, T.D. Frank and J. L. Isbell (Eds.). *Resolving the Late Palaeozoic Age in Time and Space*. Geological Society of America, Special Paper, 441: 71–82.

Jarvie, D.M., Hill, R.J., Ruble, T.E., and Pollastro, R.M., 2007. Unconventional shale-gas systems: the Mississippian Barnett Shale of north-central Texas as one model for thermogenic shale-gas assessment. *American Association of Petroleum Geologists Bulletin*, 91: 475–499.

Johnson, M. R., 1976. *Stratigraphy and sedimentology of the Cape and Karoo sequences in the Eastern Cape Province*. Unpublished PhD Thesis, Department of Geology, Rhodes University, Grahamstown, 1–267.

Johnson, M.R., van Vuuren, C.J., Hegenberger, W.F., Key, R., and Shoko, U., 1996. Stratigraphy of the Karoo Supergroup in southern Africa: an overview. *Journal of African Earth Sciences*, 23: 3–15.

Johnson, M.R., van Vuuren C.J., Visser, J.N.J., Cole, D.I., Wickens H. de V., Christie, A.D.M., Roberts, D.L., and Brandl, G., 2006. Sedimentary Rocks of the Karoo Supergroup. In: Johnson, M.R., Anhaeusser, C.R. and Thomas, R.L. (eds.). *The Geology of South Africa*. Pretoria: Geological Society of South Africa, Johannesberg/Council for Geoscience, 461–499.

Katz, B.J., 2006. Significance of ODP results on deep-water hydrocarbon exploration–eastern equatorial Atlantic region. *Journal of African Earth Sciences,* 46: 331–345.

Kuuskraa, V., Stevens, S., Van Leeuwen, T., and Moodhe, K., 2011. *World shale gas resources: An initial assessment*. Prepared for: United States Energy Information Administration, World Shale Gas Resources: An initial assessment of 14 regions outside the United States, Washington DC: US Department of Energy, 1–353. Available

online at: *http://www.eia.doe.gov/analysis/studies/worldshalegas*

Lecompte, B., Hursan, G., and Hughes, B., 2010. *Quantifying source rock maturity from logs. How to get more than TOC from Delta Log R. SPE Annual Technical Conference and Exhibition, Florence, Italy*. SPE 133128: SPE International, 10 pp. Available at: https://www.scribd.com/document/328695025/SPE-133128-MS-P-pdf

Lindeque, A., De Wit, M. J., Ryberg, T., Weber, M., and Chevallier, L., 2011. Deep crustal profile across the Southern Karoo basin and Beattie magnetic anomaly, South Africa: An integrated interpretation with tectonic implications. South Africa *Journal of Geology*, 114: 265–292.

Linol, B., De Wit, M.J., Milani, E.J., Guillocheau, F., and Scherer, C., 2015. Chapter 13: New regional correlations between the Congo, Paraná and Cape-Karoo Basins of southwest Gondwana. In: De Wit, M.J., Guillocheau, F., and de Wit, M.J.C. (eds.), *The Geology and Resource Potential of the Congo Basin*. Berlin, Heidelberg: Regional Geology Reviews. Springer-Verlag, 246–268. http://dx.doi.org/10.1007/978-3-642-29482-2_13.

Mahlstedt, N., and Horsfield, B., 2012. Metagenetic methane generation in gas shales I. screening protocols using immature samples. *Marine and Petroleum Geology*, 31(1): 27–42.

Maravelis, A., and Zelilidis, A., 2010. Organic geochemical characteristics of the Late Eocene-Early Oligocene submarine fan and shelf deposits on Lemons Island, NE Greece. *Journal of Petroleum Science and Engineering*, 9: 25–40.

Martini A.M., Walter L.M., and McIntosh J.C., 2008. Identification of microbial and thermogenic gas components from Upper Devonian black shale cores, Illinois and Michigan basins. *American Association of Petroleum Geologists Bulletin*, 92 (3): 327–339.

McCarthy, K., Rojas, K., Niemann, M., Palmowski, D., Peters, K., and Stankiewicz, A., 2011. Basic petroleum geochemistry for source rock evaluation. *Oil Field Review*, 23(2): 32–43.

McKay, M.P., Weislogel, A.L., Fildani, A., Rufus L., Brunt, R.L., David M. Hodgson, D.M., and Flint, S.S., 2015. U-PB zircon tuff geochronology from the Karoo Basin, South Africa: implications of zircon recycling on stratigraphic age controls. *International Geology Review*, 57: 393–410.

Montgomery S.L., Jarvie D.M., Bowker K.A., and Pollastro, R.M., 2005. Mississippian Barnett Shale, Fort Worth Basin, North-Central Texas: Gas-shale play with multi-trillion cubic foot potential. *American Association of Petroleum Geologists Bulletin*, 89: 155–175.

Newton, A.R., Shone, R.W., and Booth, P.W.K., 2006. The Cape Fold Belt. In: M.R. Johnson, C.R. Anhausser and R.J. Thomas (eds.). *The Geology of South Africa*. Johannesburg: Geological Society of South Africa/Council for Geoscience, 521–530.

Nuñez-Betelu, L., and Baceta, J.I., 1994. Basics and application of Rock-Eval/TOC Pyrolysis: An example from the uppermost Paleocene/lowermost Eocene in the Basque Basin, Western Pyrenees. *Munibe Natural Sciences-Natur Zientziak*, 46: 43–62.

Pángaro, F., and Ramos, V.A., 2012. Palaeozoic crustal blocks of onshore and offshore central Argentina: New pieces of the southwestern Gondwana collage and their role in the accretion of Patagonia and the evolution of Mesozoic south Atlantic sedimentary basins. *Marine and Petroleum Geology,* 37: 150–162.

Peters, K.E., 1986. Guidelines for evaluating petroleum source rock using programmed analysis. *American Association of Petroleum Geologists Bulletin*, 70: 318–329.

Peters, K.E., and Cassa, M.R., 1994. Applied source rock geochemistry. In Magoon, L.B., and Dow, W.G., (eds.), *The petroleum system – from source to trap*. American Association of Petroleum Geologists, 60: 93–120.

Rubidge, B.S., Erwin, D.H., Ramezani, J., Bowring, S.A., and de Klerk, W.J., 2013. High-precision temporal calibration of late Permian vertebrate biostratigraphy: U-Pb constraints from the Karoo Supergroup, South Africa. *Geology*, 41: 363–366.

SACS, South African Committee for Stratigraphy, 1980. In: Kent, L.E. (Compiler), *Stratigraphy of South Africa, Part 1*. Handbook Geological Survey of South Africa, Pretoria, 8: 690.

SANS ISO 7404-2, International Organization for Standardization 2009. *Methods for the petrographic analysis of coals. Part 2: Methods of preparing coal samples, 12, Pretoria: SABS Standards Division*.

SANS ISO 7404-5, International Organization for Standardization 2009. *Methods for the petrographic analysis of coal. Part 5: method of determining microscopically the reflectance of vitrinite, 13, Pretoria: SABS Standards Division.*

Smith, R., Eriksson, P., and Botha, W., 1993. A review of the stratigraphy and sedimentary environments of the Karoo-aged basins of southern Africa. *Journal of African Earth Sciences*, 16: 143–169.

Steyl, G., and van Tonder, G.J., 2013. Hydrochemical and hydrogeological impact of hydraulic fracturing in the Karoo, South Africa, Effective and Sustainable Hydraulic Fracturing, *Intech Online Journal*, 213–237. Available at: http://dx.doi.org/10.5772/56310

Suarez-Ruiz, I., Flores, D., Graciano Mendonca Filho, J., and Hackley, P.C., 2012. Review and update of the applications of organic petrology: Part 1, geological applications. *International Journal of Coal Geology*, 99: 54–112.

Svensen, H., Bebout, G., Kronz, A., Li, L., Planke, S., Chevallier, L., and Jamtveit, B. 2008. Nitrogen geochemistry as a tracer of fluid flow in a hydrothermal vent complex in the Karoo Basin, South Africa. *Geochim. Cosmochim. Acta,* 72 (20): 4929–4947.

Svensen, H., Planke, S., Chevallier, L., Malthe-Sorenssen, A., Corfu, F., and Jamtveit, B., 2007. Hydrothermal venting of greenhouse gases triggering Early Jurassic global warming. *Earth Planet. Sci. Lett.,* 256 (3/4): 554–566.

Tankard, A., Welsink, H., Aukes, P., Newton, R., and Stettler, E., 2009. Tectonic evolution of the Cape and Karoo basins of South Africa. *Marine and Petroleum Geology*: 26, 1379–1412.

Tankard, A., Welsink, H., Aukes, P., Newton, R., and Stettler, E., 2012. Geodynamic interpretation of the Cape and the Karoo basins, South Africa. *Phanerozoic Passive Margins, Cratonic Basins and Global Tectonics Maps*. 869.

Tissot, B.P., and Welte, D.H., 1978. *Petroleum Formation and Occurrence* (First Edition). New York: Springer-Verlag, (1–538).

Tissot, B., and Welte, D.H., 1984. *Petroleum Formation and Occurrence*. Berlin: Springer Verlag, 1–699.

Vengosh, A., Jackson, R.B., Warner, N., Darrah, T.H., and Kondash, A., 2014. A critical review of the risks to water resources from unconventional shale gas development and

hydraulic fracturing in the United States. *Environ. Sci. Technol.,* 47(22): 13141–13150.

Vermeulen, P.D., 2012. A South Africa perspective on shale gas hydraulic fracturing. In: McCullough, C.D., Lund, M.A., and Wyse, L. (eds.), *International Mine Water Association Symposium, Bunbury, Western Australia*. Journal of the International Mine Water Association, 149–156. Online: https://www.imwa.info/docs/imwa_2012/IMWA2012_Vermeulen_149.pdf

Viljoen, J.H.A., 1992. Lithostratigraphy of the Collingham Formation (Ecca Group), including the Zoute Kloof, Buffels River and Wilgehout River members and the Matjiesfontein Chert Bed. *South African Committee for Stratigraphy, Lithostratigraphic Series,* 22: 1–10.

Viljoen, J.H.A., 1994. Sedimentology of the Collingham formation, Karoo Supergroup, South Africa. *Journal of Geology*, 97: 167–183.

Wickens, H. de V., 1994. *Basin Floor Fan building Turbidites of the South Western Karoo Basin. Permian Ecca Group, South Africa*. PhD thesis, University of Port Elizabeth, Port Elizabeth, 1–233.

Zoback, M.D., and Arent, D.J., 2014. The opportunities and challenges of sustainable shale gas development. *Elements*, 10: 251–253.

Zou, C., Yang, Z., Pan, S., Chen, Y., Lin, S., Huang, J., Wu, S., Dong, D., Wang, S., Liang, F., Sun, S., Huang, Y., and Weng, D., 2016. Shale gas formation and occurrence in China: An overview of the current status and future potential. *Acta Geologica Sinica* (English Edition), 90(6): 1249–1283.

About the first author:

Christopher BAIYEGUNHI (Ph.D.), male, is a postdoctoral fellow at the department of Geology, University of Fort Hare South Africa. He is an active and intelligent scholar with high capacity to stimulate thoughts in academic research, a registered member of the Geological Society of South Africa, Nigerian Association of Petroleum Explorationists, and Society of Exploration Geophysicist and European Association of Geoscientists and Engineers. His current research interest focuses on sedimentology and shale gas potential of the Ecca Group, Karoo Supergroup, Eastern Cape Province of South Africa. He intend to become a renowned academic in the nearest future and aim at touching the lives of people positively in whatever capacity he might find himself. Email: cbaiyegunhi@ufh.ac.za, cbaiyegunhi@yahoo.com; mobile: +27738499853.